

1 **Correspondence:** Dr Christelle Margoum, Irstea, UR MALY, 5 rue de la Doua, CS 20244, F-

2 69625, Villeurbanne Cedex, France

3 E-mail: christelle.margoum@irstea.fr

4 Tel: + 33 4 72 20 87 11

5

6 **Running Head:** Silicone rubber rods as passive samplers for pesticides

7

8 **Calibration of silicone rubber rods as passive samplers for pesticides at two**
9 **different flow velocities: modelling of sampling rates under water boundary**
10 **layer and polymer control**

11 A. Martin †, C. Margoum* †, A. Jolivet †, A. Assoumani †, B. El Moujahid †, J. Randon ‡, M.
12 Coquery †

13 † Irstea, UR MALY, 5 rue de la Doua, CS 20244, F-69625 Villeurbanne Cedex, France

14 ‡ Univ Lyon, CNRS, Université Claude Bernard Lyon 1, ENS de Lyon, Institut des Sciences
15 Analytiques, UMR 5280, 5 rue de la Doua, F-69100 Villeurbanne, France

16 *Corresponding author: Tel: + 33 4 72 20 87 11; Fax: + 33 4 78 47 78 75; Email address: christelle.margoum@irstea.fr

17

18 **Abstract**

19 There is a need to determine time-weighted average concentrations of polar contaminants
20 such as pesticides by passive sampling in environmental waters. Calibration data for silicone
21 rubber (SR)-based passive samplers are lacking for this class of compounds. The calibration
22 data, sampling rate (R_s) and partition coefficient between SR and water (K_{sw}) were precisely
23 determined for 23 pesticides and 13 candidate performance reference compounds (PRCs) in a
24 laboratory calibration system over 14 d for two water flow velocities, 5 cm s^{-1} and 20 cm s^{-1} .
25 Results showed that an in situ exposure duration of 7 d left a SR rod passive sampler
26 configuration in the linear or curvilinear uptake period for 19 of the pesticides studied. A
27 change in the transport mechanism from polymer control to water boundary layer control was
28 observed for pesticides with a $\log K_{sw}$ of around 3.3. The PRC candidates were not fully
29 relevant to correct the impact of water flow velocity on R_s . We therefore propose an
30 alternative method based on an overall resistance to mass transfer model to adjust R_s from
31 laboratory experiments to in situ hydrodynamic conditions. We estimated diffusion
32 coefficients (D_s) and thickness of water boundary layer (δ_w) as adjustable model parameters.
33 $\log D_s$ values ranged from -12.13 to $-10.07 \text{ m}^2 \text{ s}^{-1}$. The estimated δ_w value showed a power
34 function correlation with water flow velocity.

35

36 **Keywords:** pesticides, polydimethylsiloxane, freshwaters, mass transfer model, monitoring

37

38

39

40

41

42 1 Introduction

43 The monitoring of trace levels of pesticides with a wide range of physical and chemical
44 properties is a challenge for sampling and analysis to evaluate water resource quality. The
45 variability in the discharge of pesticides into the environment, such as during flood events in
46 small agricultural watersheds, requires the development of suitable methods that take
47 temporal variations into account [1]. Passive sampling offers a promising alternative to
48 classical grab sampling. It allows the determination of representative time-weighted average
49 concentrations of contaminants, such as pesticides in freshwaters, at lower logistical and
50 analytical costs [2].

51 Passive sampling community experts recently recommended monophasic polymers (e.g.
52 silicone rubber (SR) or low density polyethylene (LDPE) as passive sampler materials of
53 choice for hydrophobic and non-ionised organic compounds [3]. These passive samplers are
54 available in a large variety of shapes: sheets, tubes, rods or coated stir bars named “Passive
55 SBSE” (Stir Bar Sorptive Extraction) [4]. Modelling of contaminant uptake mechanisms in
56 monophasic polymers, such as SR, is now well-documented for passive sampling of
57 hydrophobic contaminants (PAHs and PCBs) [5-11]. Although SRs are strongly hydrophobic
58 [12], they can extract organic compounds with a broad range of polarities ($\log K_{ow} > 1-2$) from
59 water but only a few studies have focused on pesticides [13-17]. Sorption properties of SRs
60 for polar contaminants have mainly been assessed by determining partition coefficients
61 between the SR and water at equilibrium (K_{sw}), but if equilibrium is not attained, the
62 determination of representative time-weighted average concentrations in water requires
63 determining uptake kinetic parameters such as sampling rates (R_s) or diffusion coefficients
64 (D_s) in the SR for every compound studied [18-20]. The uptake kinetic parameters are
65 dependent on the variation of environmental factors including water flow velocity [5, 7, 8],

66 temperature, salinity [21] and biofouling [22, 23]. To correct for environmental variability,
67 and especially water flow velocity, R_s can be estimated from the dissipation rates of
68 performance reference compounds (PRCs) with which the passive sampler is spiked
69 beforehand [24]. A second method, described by Estoppey et al. [7] with SR sheets, is based
70 on correction factors derived from a power function relationship between the compound
71 uptake and water flow velocity. This new method was introduced to correct PCB
72 concentrations among sites with great differences in water flow velocity, where PRC-based R_s
73 overcorrected the impact of varying flow velocities. Estoppey et al. [8] recently improved
74 their method for PCBs by using a simple linear correlation between R_s and flow velocity. For
75 SRs, a close agreement between this second method and PRC correction was reported for
76 flow velocities from 10 cm s⁻¹ to 60 cm s⁻¹ [8], and a similar linear correlation was observed
77 by O'Brien et al. [25] using a passive flow monitor. This method has the advantages of being
78 accessible by the operator applying passive samplers, less time consuming, less expensive
79 than PRC-based methods and not influenced by uncertainties in log K_{sw} and R_s determination
80 [8].

81 The determination of R_s requires a calibration experiment with a constant concentration of
82 contaminants and controlled experimental parameters (constant temperature and adjustable
83 flow velocity) [26]. For SRs, few calibrations have been conducted for pesticides and
84 especially for polar pesticides [6, 14, 17, 27]. These calibration studies highlighted the need
85 for an experimental design adapted to pesticide properties with short exposure monitoring
86 (<15 d). Emelogu et al. [27] quantified urea herbicide in field studies with SR-based passive
87 samplers, but lacked calibration data to convert mass accumulated by the SR into water
88 concentration.

89 The main goal of this study was to determine R_s and K_{sw} for 24 polar and non-polar pesticides
90 ($0.6 < \log K_{ow} < 5.5$) with an experimental calibration, in order to estimate an appropriate

91 deployment period for linear uptake in freshwaters. We also assessed the impact of water flow
92 velocity on the uptake of pesticides. The use of 13 deuterated pesticides as PRC candidates
93 was evaluated to correct R_s for differences in flow velocity. The kinetic variables were
94 determined using a home-made calibration system with adjustable water flow velocity and a
95 diffusive source of pesticides. The theoretical model of overall resistance to mass transfer [28]
96 was first applied to estimate D_s values. In a second step, we then used this model to predict R_s
97 of pesticides for other water flow velocities in order to simplify the calculation of time-
98 weighted average concentrations in different field applications.

99

100 2 Mass transfer resistance model in silicone rubber- 101 based passive samplers

102 The mass transfer of contaminants into a passive sampler depends mainly on both the
103 characteristics of the device and the physical and chemical properties of the sampled analytes,
104 but it depends also on environmental factors. We focused only on the theory for membrane-
105 free or monophasic samplers, such as SR plates. In this configuration, the exchange process is
106 driven by different transport mechanisms involving transport of the compound by diffusion
107 through the water, diffusion across the thickness of the receiving phase/ polymer. The
108 transport across the biofilm layer for long exposure in water was neglected in the present
109 work. Each transport mechanism contributes to the resistance to mass transfer ($1/k_o$),
110 calculated using Eq. 1, with k_w and k_s as the mass transfer coefficients in the water and the SR
111 polymer respectively, and K_{sw} the silicone-water partition coefficient [26, 29, 30].

$$\frac{1}{k_o} = \frac{1}{k_w} + \frac{1}{K_{sw}k_s} \quad (1)$$

112 According to Greenwood et al. [26] and Huckins et al. [28], the individual mass transfer for a
113 specific compound is related to the ratio of the compound's diffusion coefficient (D) and the
114 thickness (δ) of each compartment (water or SR, respectively noted with subscripts w and s)
115 contributing to k_o . The mass-transfer coefficients for each compartment are calculated as
116 follows (Eq. 2 and Eq. 3):

117

$$k_s = \frac{D_s}{\delta_s}, \quad (2) \quad k_w = \frac{D_w}{\delta_w}. \quad (3)$$

118 If diffusion occurs from both sides for a plate configuration of a SR-based passive sampler,
119 the barrier thickness (δ_s) is considered as the half-thickness. Using the very simplified
120 approach of Zhao et al. [31], where a linear concentration profile is assumed within the
121 polymer cylinder or rod configuration, the barrier thickness (δ_s) is considered as the half-
122 diameter or radius. For the water compartment, the notion of water boundary layer (WBL) of
123 thickness δ_w was assumed for convenience, considering the complexity of the hydrodynamics.
124 In this work, we chose to use a mass transfer resistance model with linear concentration
125 profiles in both the WBL and the SR. It is a simple and approximated model, contrary to the
126 two-phase Fickian model [29] (considering a time-dependent D_s and resulting in non-linear
127 diffusion profiles in the polymer) that would lead to more accurate results.

128 Assuming that elimination and uptake of compounds obey first-order kinetics (isotropic
129 exchanges), the uptake of compounds in an SR-based passive sampler over time with constant
130 ambient water concentration (and free of compounds at deployment), is described by Eq. 4:

$$C_s(t) = C_w K_{sw} (1 - \exp(-k_e t)), \quad (4)$$

131 where C_s (ng L^{-1}) is the concentration of the compound accumulated in the receiving phase;
132 C_w (ng L^{-1}) the concentration of the compound in the water phase, and t (d) the duration of

133 exposure. Elimination and uptake rate constants, respectively k_e (d^{-1}) and k_u (d^{-1}) are linked by
134 a proportional constant K_{sw} ($L L^{-1}$), the silicone-water partition coefficient. It is described by
135 the ratio of concentration at equilibrium of the compound in the sampler $C_{s,eq}$ ($ng L^{-1}$) to the
136 concentration at equilibrium of the compound in the water phase $C_{w,eq}$ ($ng L^{-1}$). The
137 elimination rate constant k_e is expressed by:

$$k_e = \frac{R_s}{K_{sw} V_s} = \frac{k_o A}{K_{sw} V_s}, \quad (5)$$

138 where V_s (L) is the volume of the receiving phase, R_s is the sampling rate ($L d^{-1}$) and A (cm^2)
139 is the exposed surface area of the sampler. The calculation of time of sorption half-
140 equilibrium ($t_{1/2} = \ln 2 / k_e$) is also used to describe the calibration regime as linear ($t < t_{1/2}$),
141 curvilinear ($t_{1/2} < t < 4t_{1/2}$) or equilibrium ($t > 4t_{1/2}$) state for the exposure period (t) [28].
142 Combining Eq. 1, Eq. 2, Eq. 3 and Eq. 5, and neglecting biofilm resistance, R_s , based on the
143 properties of the compounds, is estimated by:

$$R_s = \frac{A}{\frac{\delta_w}{D_w} + \frac{\delta_s}{K_{sw} D_s}}. \quad (6)$$

144 3 Materials and methods

145 3.1 Chemicals

146 The 24 pesticides selected, including two metabolites, covered a broad polarity range ($0.6 <$
147 $\log K_{ow} < 5.5$) and were listed in Table 1. Among them, 13 additional deuterated pesticides
148 were used as PRCs (SI-1). Pesticides, PRCs and one internal standard (diuron-d6) used for
149 quantification were purchased from Dr Ehrenstorfer (Augsburg, Germany) and Sigma Aldrich
150 (Saint-Quentin Fallavier, France). Acetone and dichloromethane for pesticide residue
151 analysis, UHPLC grade acetonitrile, ethyl acetate and methanol were purchased from
152 Biosolve (Dieuze, France). LC-MS grade formic acid (purity 98%) was supplied by Waters

153 (Guyancourt, France). Ultrapure water was obtained using a Millipore water purification
154 system equipped with an LC-Pak cartridge (Billerica, MA, USA). Nitrogen gas (purity
155 99.995%) used for thermal decontamination was purchased from Messer (Saint-Georges-
156 d'Espéranche, France).

157 3.2 Passive samplers

158 The passive samplers used in this study were made of SR shaped into small rods. The shape
159 of rod was preferred to the classic sheet because of the convenience of handling and storage,
160 the lower volume of solvent required for back extraction and the possibility to use
161 thermodesorption (TD)-GC/MS analysis. Translucent SR was obtained as flexible cord from
162 Goodfellow (Lille, France). This SR had been selected in an earlier study for its sorption
163 properties for pesticides [13]. The SR was cut with a clean cutter blade into rods (20×3 mm),
164 with a surface area of 2.03 cm^2 and a volume of $141 \mu\text{L}$. Silicone rubber rods (SR rods) were
165 selected by weight ($165 \text{ mg} \pm 2.5\%$, $d = 1.2$) to ensure repeatability.

166 Before use, SR rods were chemically and thermally cleaned to remove most residues such as
167 oligomers that could interfere with the instrumental analysis [13]. First the SR rods were
168 chemically conditioned by immersion in dichloromethane/methanol (50/50, v/v) under
169 sonication for 15 min. They were then wiped with a lint-free tissue and dried at $70 \text{ }^\circ\text{C}$ for 1 h,
170 and thermally treated in a Gerstel tube conditioner TC (Mülheim a/d Ruhr, Germany) under a
171 nitrogen flow (75 mL min^{-1}) with a temperature ramp of $10 \text{ }^\circ\text{C min}^{-1}$ to $300 \text{ }^\circ\text{C}$ maintained
172 constant for 1 h.

173 Cleaned SR rods ($n = 34$) were preloaded with PRCs by agitation at 600 rpm for 48 h in
174 650 mL of ultrapure water spiked with a mixture of 13 PRCs (water concentrations ranging
175 from 150 to $220 \mu\text{g L}^{-1}$). The SR rods were then gently rinsed with ultrapure water, dried with
176 a lint-free tissue and stored at $-18 \text{ }^\circ\text{C}$ until deployed in the calibration system. Before

177 deployment each SR rod was inserted into a stainless steel spring (30×5 mm, wire diameter
178 0.4 mm) to simplify handling.

179 3.3 *Characteristics of the calibration system*

180 The calibration system was custom-made (Colas & Gire, Saint-Genis-les-Ollières, France). It
181 consisted of a stainless steel cylindrical tank (diameter 40 cm, height 35 cm), with a stirring
182 system and hooks fixed on the inner wall of the tank at 4 levels, each level enabling the
183 experimenter to expose 8 SR rods or 8 SR dosing sheets (Figure 1). Two copper wire hoops
184 were fitted in the middle of the tank. Eight magnetic stir bars, wrapped in aluminium foil,
185 were fixed on the copper wire between each hook; in this way the SR rods in their springs
186 were retained magnetically at each position. The stainless steel tank was filled with 31.4 L of
187 tap water and placed in a thermostatic bath at 20 °C. The tank was covered with an aluminium
188 plate to prevent evaporation and photo-degradation in the water compartment. A Tinytag self-
189 recording thermometer (Gemini Data Loggers Ltd, Chichester, United Kingdom) was
190 immersed in the thermostatic bath to continuously follow the water temperature during the
191 experiment.

192 Stirring was done by a four-blade motor-driven propeller composed of an agitator motor
193 (RZR 2020 Control from Heidolph Instrument, Schwabach, Germany) and a propeller with a
194 diameter of 10 cm (type R1345 from IKA, Staufen, Germany). The rotation generated a water
195 flow velocity near the SR rod positions (set at 5 and 20 cm s⁻¹). These flow velocities were
196 measured with a propeller-type current meter (Streamflo430, Nixon, Cheltenham, United
197 Kingdom) in the same way for all positions in the tank. All dimensions of the calibration
198 system are availables in SI-2.

199 Constant concentrations of pesticides of about 1 µg L⁻¹ in the water were ensured by two
200 methods. Some polar pesticides (CBZ, CTU, DIU, IMD, IPU, NFZ) (Table 1) were directly

201 added to the water using 5 mL of a highly concentrated solution in acetone. For more apolar
202 pesticides, spiked SR sheets acted as diffusive contaminant sources in the water [5, 10]. Eight
203 SR sheets ($2 \times 7.5 \times 0.3$ cm, Goodfellow) were fixed with hooks at the bottom of the tank.
204 The total volume of the dosing sheets was 20 times that of the SR rods, ensuring that
205 depletion caused by uptake would be negligible. Before being spiked, the sheets were cleaned
206 by shaking in ethyl acetate and then rinsing in ultrapure water [32]. The quantity of pesticides
207 absorbed by the sheets was assessed with partition coefficients determined by Martin et al.
208 [13]. For the spiking step, the SR sheets were placed in a bottle containing 2.5 L of ultrapure
209 water contaminated with 5 mL of highly concentrated pesticide solutions (concentrations
210 ranging from 56 to 923 mg L⁻¹ in acetone) and the bottle was shaken for 72 h at 300 rpm.
211 Before the exposure of PRC preloaded passive samplers, the system was run for 72 h to allow
212 the stabilization of the pesticide concentrations by reaching equilibrium between water and
213 the spiked sheets for all the compounds (including added polar pesticides).

214 3.4 Experimental design

215 Two calibration experiments lasting 14 days were performed with SR rods spiked with PRCs
216 to simultaneously follow uptake and elimination of compounds at an effective water flow
217 velocity of 5.5 ± 2.3 cm s⁻¹ ($n = 14$) and 19.9 ± 3.5 cm s⁻¹ ($n = 19$). A total of 20 SR rods were
218 exposed for each experiment. Three SR rods spiked with PRCs were analysed to determine
219 the initial concentrations of PRCs. The first SR rod was removed from the tank 30 min after
220 the beginning of the experiment and then after 1, 2, 4, 8 h, and 1, 2, 3, 4, 5, 6, 7, 10, 14 days.
221 Additional triplicates of SR rods were also exposed and analysed to evaluate overall
222 repeatability for both uptake of pesticides and elimination of PRCs. The triplicates of SR rods
223 exposed are detailed in the spreadsheet file (SI-7) compiling results of the calibration
224 experiments. During the experiments, a 10 mL water sample was taken in an amber flask

225 every time a SR rod was collected from the tank to measure concentrations of pesticides. All
226 the SR rods and water samples were stored at $-18\text{ }^{\circ}\text{C}$ before analysis. Moreover, total organic
227 carbon (TOC) was measured at the start and the end of each experiment in acidified water
228 samples (HCl 2N, 1%, v/v) with TOC analyser (multi N/C® 3100, Analytik Jena) using
229 thermal oxidation (850°C) and NDIR (Non-Dispersive Infrared) sensor.

230 3.5 Analytical procedure

231 Pesticides were desorbed from SR rods by chemical extraction according to the protocol
232 developed by Martin et al. [13]. The solvent back-extraction recoveries of this step were
233 between 60 and 98% depending on the compounds (listed in Table 1). Briefly, SR rods were
234 rinsed with ultrapure water, wiped with lint-free tissue and stored at $-18\text{ }^{\circ}\text{C}$. Before analysis
235 the pesticides absorbed in the SR rods were desorbed in 200 μL of acetonitrile/methanol
236 (50/50) for 15 minutes under sonication. Finally, 40 μL of the desorbate was added to 150 μL
237 of ultrapure water and 10 μL of a diuron-d6 solution ($200\text{ }\mu\text{g L}^{-1}$) to prepare the extract for
238 analysis by UHPLC-MS/MS (Nexera X2 UHPLC system, Shimadzu and API 4000, AB
239 Sciex). For calibration experiments, the analysis of the water samples was performed by direct
240 injection. An aliquot of water of 1 mL was spiked with diuron-d6 at a concentration of $10\text{ }\mu\text{g}$
241 L^{-1} as for the SR rod extract analysis. Chromatographic parameters, limit of quantification
242 (LOQ) and settings for MS/MS (SI-1) analysis are reported elsewhere by Martin et al. [13].

243 4 Results and discussion

244 4.1 Monitoring of experimental parameters

245 During the two 14-day exposure experiments, the mean water temperature recorded was 19.7
246 $\pm 0.5\text{ }^{\circ}\text{C}$. Considering two measures per experiment and the results of both experiments, we
247 observed a slight variation of pH, from 7.9 ± 0.6 at the start of the calibration to 8.6 ± 0.1 at

248 the end. No influence of pH on the properties of the selected pesticides or the range of
249 fluctuation was expected. A mean value of TOC for the two experiments was measured at 3.5
250 $\pm 1.1 \text{ mg L}^{-1}$ ($n = 4$).

251 The mean pesticide concentrations in the water of the tank ranged from $0.4 \text{ }\mu\text{g L}^{-1}$ to $3.1 \text{ }\mu\text{g L}^{-1}$
252 (Table 1). We opted to work at higher concentrations for some pesticides (TBZ at $23.9 \text{ }\mu\text{g L}^{-1}$
253 1 , FNT at $24.1 \text{ }\mu\text{g L}^{-1}$ and PCM at $9.6 \text{ }\mu\text{g L}^{-1}$) that had a higher LOQ or could be partly
254 degraded or absorbed by our experimental calibration system. The concentrations of the 23
255 pesticides remained stable (RSD between 8% and 27%, $n = 30$). By contrast, a higher RSD
256 was obtained for PCM (41%), which may have been partly degraded (aqueous hydrolysis
257 DT_{50} of PCM: 25 d). Nevertheless, the SR sheets added into the tank acted as a contaminant
258 source as expected for the other pesticides. The PRC concentrations in the water of the tank at
259 the end of either experiment were below LOQ.

260 4.2 Determination of kinetic parameters

261 Considering the two experiments, repeatability of sorbed mass on triplicates of SR rods
262 sampled in experiments, expressed as RSD ($n = 3$), ranged from an average value of 3.6% for
263 dimethomorph (DMM) to 14.5% for spiroxamine (SPX), except for PCM (21.5 %). These
264 RSD values take into account the accumulation of target pesticides in the SR rods, the liquid
265 desorption process and the UHPLC-MS/MS analysis. We therefore excluded PCM from this
266 study owing to high variability in uptake into SRs and in the water of the tank (cf. §4.1). All
267 calibration results are detailed in an additional spreadsheet (SI-7).

268 For each pesticide, the concentration factor (C_s/C_w) was calculated according to the ratio
269 between the concentration in the SR rod (ng L^{-1}) and the mean concentration in water (ng L^{-1})
270 from the beginning of the experiment to the same sampling time. The concentration factors of
271 the pesticides for various time periods were fitted to a first order uptake model (Eq. 7 derived

272 from Eq. 4 and Eq. 5) using R_s and K_{sw} as adjustable variables. We optimised the sum of the
273 squared differences between the experimental and calculated values to a minimum using non-
274 linear regression with XLSTAT software (version 2015.3.01.19703). The RSD values of the
275 kinetic parameters were calculated using the derivative of the function for each parameter.

$$\frac{C_s}{C_w}(t) = K_{sw} \left(1 - \exp\left(-\frac{R_s t}{K_{sw} V_s}\right) \right). \quad (7)$$

276 We obtained satisfactory coefficients of determination (r^2) of fitted data with the first order
277 uptake model, ranging from 0.938 to 0.993. The calculation of parameters (R_s , K_{sw} , $t_{1/2}$) took
278 into account solvent back extraction recoveries determined in Martin et al. [13]. The
279 calculated parameters are detailed in Table 1, and the fitted curves are illustrated in SI-3. The
280 constants of elimination of pesticides in uptake experiments ($k_{e\ up}$) were calculated using their
281 associated R_s and K_{sw} values according to Eq. 5.

282 The times of sorption half-equilibrium ($t_{1/2}$) ranged from 0.2 d for DCA, reaching equilibrium
283 very quickly in SR rods, up to nearly 15.2 d for CPE at 5 cm s⁻¹. Comparing DCA properties
284 with DMM, which has an equivalent log K_{ow} , the fast uptake kinetic of DCA may be related to
285 its low molecular volume (121 Å³ and log K_{ow} of 2.69). DMM has a larger molecular volume
286 (342 Å³ and log K_{ow} of 2.68), and we observed a longer $t_{1/2}$ (6.4 d) at 5 cm s⁻¹. Thus, mainly
287 curvilinear and equilibrium patterns were observed for the uptake of pesticides in SR rods at 5
288 cm s⁻¹ for 14 d exposure. Equilibrium state was reached more frequently in the calibration
289 experiment at 20 cm s⁻¹. The impact of flow velocity is discussed in section 4.3.

290 According to low flow velocities measured near passive samplers in freshwaters (close to 5
291 cm s⁻¹ with a deployment system), we found that an in situ exposure duration of 7 d was a
292 good compromise in this SR rod passive sampler configuration to stay within the linear or
293 curvilinear uptake period for 19 out of 23 pesticides ($4t_{1/2} > 7$ d except for DCA, FNT, MTC
294 and TBZ).

295 Those $t_{1/2}$ values are greater than those previously reported for a selection of 19 pesticides
296 with “Passive SBSE” [4]. The authors obtained a $t_{1/2}$ ranging from 1.5 to 4 d in an experiment
297 with flow velocity at 2.5 cm s^{-1} . This difference is because of the use of different geometries
298 (area and volume) between the two passive samplers ($A/V=17.0 \text{ cm}^{-1}$ and 14.3 cm^{-1}
299 respectively for Passive SBSE and SR rod) [9] or differences in diffusion coefficients (D_s).
300 Pesticides potentially diffuse into the half-diameter of SR rods (1.5 mm), whereas the
301 thickness of the SBSE coating is only 1 mm.
302 Calculated sampling rates (R_s) for the two experiments are reported in Table 1 with their
303 relative standard deviations (RSD). Sampling rates ranged between 0.039 mL d^{-1} (IMD) and
304 812 mL d^{-1} (CPE), with RSD ranging from 8% to 27%. In comparison, “Passive SBSE”
305 exhibited lower R_s values by a mean factor of 4.7 for 19 pesticides studied in common,
306 excluding DCA, which differed by a factor of 68 [4]. Differences in D_s due to a specific SR
307 formulation could explain this difference for DCA, as no differences in sorption at
308 equilibrium were found for this compound by Martin et al. [13].
309 The partition coefficients calculated in both experiments were compared with results obtained
310 on the same SR in an earlier study by sorption isotherm experiments reported by Martin et al.
311 [13] (SI-4). For pesticides with $\log K_{sw} < 3$, K_{sw} values obtained in the present study were 1.8
312 to 8.9 times greater than K_{sw} previously determined. Martin et al. [13] suggested a possible
313 adsorption of the pesticides on the SR following a non-linear sorption isotherm depending on
314 water concentration (Freundlich model). However, $K_{sw \text{ Freundlich}}$ calculated with the mean
315 concentration in water does not match the K_{sw} values obtained in the present study. This
316 difference could be due to different experimental approaches and calculation methods, or to
317 the influence of water characteristics on adsorption (Evian® water vs. tap water). We adopted
318 K_{sw} values derived from Eq. 7 in the experiment at 20 cm^{-1} as reference values (Table 1),
319 because equilibrium state was reached more frequently in calibration experiments at 20 cm s^{-1}

320 than at 5 cm s^{-1} for most pesticides after 14-d exposure (Cf. § 4.3), leading to more accurate
321 values.

322 4.3 Impact of flow velocity on uptake of pesticides

323 As predicted by the theoretical model (Cf. § 2.0), a correlation of sampling rate, expressed as
324 $\log R_s$ normalised per 100 cm^2 , with $\log K_{sw}$ should highlight the control of uptake kinetics by
325 the WBL or by the polymer. This change in transport mechanism was expected for
326 hydrophobic compounds with $\log K_{ow}$ in the range 3.5–5 [11, 33]. For hydrophilic compounds
327 theoretically under polymer control ($R_s \approx AK_{sw}D_s/\delta_s$), R_s values were expected to increase
328 with increasing K_{sw} . On the contrary, for more hydrophobic compounds, such as PCBs and
329 PAHs (with $\log K_{ow} > 3.3$) not investigated in the present study, R_s values were expected to be
330 constant and slowly decrease with increasing K_{sw} [5], in accordance with WBL control theory
331 ($R_s \approx AD_w/\delta_w$) (compounds with high K_{sw} also have a lower D_w).

332 In our experiments (Figure 2), for polar pesticides with a low affinity for SR, we observed
333 that the R_s values increased with increasing values of $\log K_{sw}$ up to around 3, whereas for
334 more hydrophobic pesticides, R_s remained constant irrespective of the $\log K_{sw}$ values.
335 The plot of $\log R_s$ at the two velocities (Figure 2) shows similar R_s values for polar pesticides,
336 and highlights a significant separation of the two curves at $\log K_{sw}$ around 3.3, defined as
337 graphical intersection of tangents from both ends, with higher values of R_s for the experiments
338 at 20 cm s^{-1} . This change in behaviour demonstrates the impact of hydrodynamics on the
339 thickness of the WBL and on R_s values. A higher flow velocity leads to a thinner WBL,
340 resulting in an increase in R_s proportional to $1/\delta_w$. To our knowledge, this is the first time that
341 the change from polymer control to WBL control for $\log K_{sw} > 3.3$ has been experimentally
342 confirmed with polar and non-polar compounds ($0.6 < \log K_{ow} < 5.5$) using different flow

343 velocities. This result is consistent with those of Assoumani et al. [4], suggesting a WBL
344 control for pesticides with $\log K_{ow}$ above 3.3 (FNT) in “Passive SBSE” (coated with SR).

345 4.4 PRCs desorption kinetics: isotropic exchanges?

346 The elimination of PRC obeys first-order kinetics described by:

$$m_s(t) = m_0 \exp(-k_{e\ PRC} t), \quad (8)$$

347 where m_s (ng) is the mass of PRC remaining in the receiving phase of the sampler, and m_0
348 (ng) is the initial mass of spike PRC in the receiving phase. The repeatability of mass
349 measurement on triplicates of SR rods sampled in experiments was similar for the release of
350 13 PRCs and for the uptake of pesticides (RSD from 4.3% to 12.2%). The release of PRCs
351 from the SR rods was fitted by nonlinear regression of PRCs fractions ($f = m_s(t)/m_0$)
352 remaining in the SR rod as a function of exposure time (t) using Eq. 8 (XLSTAT), with the
353 elimination constant ($k_{e\ PRC}$) as an adjustable parameter (fitted curves are available in SI-3).
354 Unlike in uptake experiments, not all coefficients of determination (r^2) were satisfactory
355 (ranging from 0.15 to 0.91). Some PRCs (ATZ-d5, CBZ-d4, IPU-d6, MTC-d6 at 5 cm s^{-1} and
356 CBZ-d4, FNT-d6 at 20 cm s^{-1}) seemed to obey elimination kinetics with an inflexion point (or
357 two slopes) that could not be described by Eq. 8. This was also observed for some compounds
358 with another passive sampler (POCIS) by Morin et al. [34]. Accordingly only PRCs obeying
359 first order kinetics were considered for the present study and the data for above mentioned
360 PRC were removed.

361 Several hypotheses can be ventured to explain these deviations from the first order kinetic
362 model. Adsorption on SR could be involved instead of absorption for these strongly polar
363 PRCs. Another explanation is that the geometry of SR rods with a half-thickness of 1.5 mm
364 makes them thicker than the silicone plates (0.25 mm), for which isotropic exchanges have
365 been demonstrated [5]. It is possible that the two-phase Fickian model was more adapted in

366 this case with a time-dependency of D_s [29, 35]. It may be that the distribution of PRCs within
367 this thicker SR-based passive sampler was not homogeneous because SR rods were preloaded
368 with PRCs without methanol, which allows fast and homogeneous equilibrium by swelling
369 the polymeric structure [36].

370 Calculated values of k_e $_{PRC}$ for the two experiments are reported in Figure 3. RSD ranged from
371 7% to 34% similarly to k_e $_{up}$ derived from the uptake experiments.

372 The use of several pairs of deuterated (PRCs) and non-deuterated pesticides allowed direct
373 comparison of the uptake and release processes. We opted to use the graphical comparison of
374 uptake/release instead of checking the equality of elimination constants (k_e $_{up}$ and k_e $_{PRC}$), due
375 to different calculation methods (k_e $_{up}$ was calculated from Eq. 5. and k_e $_{PRC}$ from Eq. 8. with
376 lower r^2). We considered a confidence interval of 10% for the intersection of uptake/release:
377 isotropic exchanges were thus validated for an intercept between 40% and 60%.

378 As shown in Figure 3, curves describing the uptake of CPM and LINU and the release of
379 CPM-d6 and LINU-d6 at 5 cm s^{-1} intersect at about 50% of the concentration interval,
380 indicating that the exchange process is isotropic. These profiles were observed for the
381 following deuterated analogues: ATC, CPM, CPE, FNT, and LINU (SI-3). Isotropic exchange
382 of FNT and FNT-d6 with “Passive SBSE” was also confirmed by Assoumani et al. [4] by
383 comparison of k_e values determined by elimination experiments for the two compounds.
384 Therefore, regarding data at 5 cm s^{-1} , the release of the 5 selected PRCs seems pertinent for
385 the correction of R_s in in situ applications.

386 In Figure 4, the $\log k_e$ $_{PRC}$ at the two flow velocities are plotted against $\log K_{sw}$ of non-
387 deuterated corresponding pesticides. A change of transport mechanism is again highlighted by
388 a global increase and then a decrease in k_e $_{PRC}$ with increasing K_{sw} values. However, in
389 contrast to uptake, no differences in the release of hydrophobic PRCs (k_e $_{PRC}$) (ATC, CFV,
390 CPM, CPE, DFF) were observed between the two flow velocities studied (Figure 4). This is

391 surprising considering the impact of flow velocity on uptake for these hydrophobic pesticides.
392 The cause of this discrepancy might arise from (i) a non-isotropic exchange for the two
393 velocities or (ii) ill-suited design of the calibration system for the elimination experiments.
394 The graphical comparison of uptake/release of PRCs at 20 cm s^{-1} showed non-isotropic
395 exchange for all pesticides; the uptake was faster than the release of PRCs (SI-3). The
396 alternative explanation is that the static calibration system design (without continuous renewal
397 of water) was not suited to following elimination kinetics.
398 Hence it is difficult to conclude on the use of selected deuterated pesticides as PRC candidates
399 in this study to take into account variation of flow velocity for R_s correction. Other
400 experiments in continuous flow calibration systems will be needed to validate this statement.
401 Considering these results from PRCs, we propose an alternative method based on an overall
402 resistance to mass transfer model to adjust R_s from laboratory experiments to other
403 hydrodynamic conditions by measuring in situ flow velocity.

404 4.5 *Application of the overall resistance to mass transfer model*

405 We first applied the overall resistance to mass transfer model on our experimental results. The
406 application of Eq. 6 required knowledge of diffusion parameters (D_w and D_s) for the pesticides
407 studied. Diffusion coefficients in water (D_w) were calculated using the method of Hayduk and
408 Laudie [37] from the molar volume of pesticides (SI-5). We chose this method according to
409 the recommendation of the US Environmental Protection Agency and the conclusions of
410 Pintado-Herrera et al. [19]. Experimental D_s values in SR are scarce in the literature, and have
411 been estimated only for a few classes of contaminants (PCBs and PAHs [20], PBDEs [18] and
412 emerging contaminants [19]) and unfortunately not determined for pesticides. We therefore
413 opted to estimate D_s values for pesticides by simultaneously fitting the data at the two flow

414 velocities to the overall resistance to mass transfer model. The WBL thickness (δ_w), not
415 available by direct measurement, was defined as an adjustment factor for the model.
416 To estimate the initial δ_w parameters for the model, we used the approximation of a theoretical
417 WBL control model ($R_s \approx AD_w / \delta_w$) with six pesticides that had $\log K_{sw} > 3.3$ and were
418 considered in WBL control (FNT, CFV, CPM, SPX, DFF, CPE) for both experiments. We
419 obtained δ_w values of 60 μm at 5 cm s^{-1} ($\delta_{w5\text{ ini}}$) and 19 μm at 20 cm s^{-1} ($\delta_{w20\text{ ini}}$). These values
420 are in the range of typical values (from a few μm to 1 mm) reported by Huckins et al. [28] for
421 SPMD.
422 We then used R_s and K_{sw} for all pesticides at the two flow velocities ($n = 48$) to calculate more
423 accurate δ_w values (δ_{w5} and δ_{w20}) and D_s values for 23 pesticides according to Eq. 6. Predicted
424 R_s values were fitted simultaneously to the experimental R_s values with adjustable parameters
425 (δ_w values and D_s values) by minimising the sum of the squares of the residuals weighted by
426 the average of the residuals with the “optim” function of R software (version 2.15.2) and a
427 limited memory algorithm for bound constrained optimisation (L-BFGS-B). The initial values
428 of adjustable parameters were $\delta_{w\text{ ini}}$ values and a $\log D_s$ value of $-11\text{ m}^2\text{ s}^{-1}$ for all pesticides
429 (approximated mean value for PAHs and PCBs as initial parameters), and lower and upper
430 bounds were respectively 0 and 1000 mm for δ_w , and -10 and -14 for $\log D_s$.
431 Predicted R_s values (normalised to 100 cm^2) adjusted to our experimental data were plotted
432 against $\log K_{sw}$ (Figure 5). Estimated δ_w values ($\delta_{w5} = 43\text{ }\mu\text{m}$ and $\delta_{w20} = 10\text{ }\mu\text{m}$) were slightly
433 lower than those evaluated initially. Estimated $\log D_s$ for pesticides are given in Table 1.
434 Estimated $\log D_s$ values in the present study were in the range -12.13 (IMD) to -10.07 (CPE)
435 $\text{m}^2\text{ s}^{-1}$. The lowest $\log D_s$ for pesticides ($-12.13\text{ m}^2\text{ s}^{-1}$) was for IMD, the most hydrophilic
436 compound studied ($\log K_{ow} = 0.6$) with the lowest affinity for SR ($\log K_{sw} = 0.71$). By
437 contrast, the highest $\log D_s$ was for CPE, the second most hydrophobic pesticide ($\log K_{ow} =$

438 4.7) with the highest affinity for SR ($\log K_{sw} = 4.60$). The most hydrophobic pesticide, SPX
439 ($\log K_{ow} = 5.5$), also had a high molar volume reported to influence the diffusion of
440 compounds in polymers [20, 38] and resulting in a decreased diffusivity in SR. Other trends
441 of the diffusion coefficients related to chemical structures are illustrated in SI-6 with $\log D_s$
442 plotted to molar volumes and molar mass.
443 This is a first evaluation of D_s values for pesticides using calibration data instead of direct
444 measurement. They therefore need to be validated with further experiments. In regard to other
445 experimental values for PAHs and PCBs for another SR formulation (supplied by Altec) [20],
446 ranging from -9.8 to $-11.0 \text{ m}^2 \text{ s}^{-1}$; our data seem reasonable. In comparison, diffusion
447 coefficient values for the studied pesticides were lower and with a wider range (2 orders of
448 magnitude) than for PCBs and PAHs (1 order of magnitude).

449 4.6 *Modelling of the influence of water flow velocity on sampling rates*

450 The knowledge of D_s for each pesticide and δ_w values related to flow velocity enabled us to
451 estimate R_s for other hydrodynamic conditions. Also, the change from the polymer control to
452 the WBL control could be predicted. This model aims at estimating δ_w by a correlation related
453 to a hydrodynamic parameter such as water flow velocity. Such a correlation was proposed by
454 Estoppey et al. [7, 8] for PCBs by in situ passive sampler exposures using LDPE and SR
455 plates.

456 Our estimated δ_w values for two different measured flow velocities were insufficient to
457 demonstrate such a correlation; we therefore used calibration data for which water flow
458 velocities were only estimated to determine complementary δ_w values. The study of Rusina et
459 al. [5] describes calibration experiments for PAHs and PCBs with SR flat plate passive
460 samplers at two calculated flow velocities (Exp A = 0.14 cm s^{-1} and Exp B = 9 cm s^{-1}),
461 assuming that uptake was controlled by diffusion in the WBL in both cases. We applied the

462 overall resistance to mass transfer model with the available experimental values of D_s for
463 PAHs and PCBs [20]. The estimated δ_w values were $\delta_{w,0.1} = 412 \mu\text{m}$ and $\delta_{w,9} = 27 \mu\text{m}$. In
464 quasi-static hydrodynamics conditions (0.14 cm s^{-1}), the WBL thickness was more than 7
465 times greater than at 5 cm s^{-1} in our experiment.

466 The estimated δ_w values from the two studies ($n = 4$) were plotted against the flow velocities
467 (v) reported in experiments in Figure 6. A power function correlation was observed between
468 δ_w values and v ($n = 4$, $\delta_w = 111.6 v^{-0.71}$, $r^2 = 0.98$). Such a correlation was indirectly
469 demonstrated by Estoppey et al. [7] with power function relations between amounts of PCB
470 accumulated and flow velocity in the range 1.9 to 37.7 cm s^{-1} . They then provided individual
471 linear correlations for 6 PCBs between PRC-based R_s and water flow velocities above 10 cm
472 s^{-1} for SR: assuming that PCB uptake was under WBL control, the R_s is proportional to $1/\delta_w$,
473 which was indirectly linked to v . Our results confirm that this relationship could also be
474 approximated by a linear correlation for flow velocities above 5 cm s^{-1} ($n = 3$, $\delta_w = -2.1 v +$
475 51 , $r^2 = 0.93$).

476 These results acquired using different SR based passive sampler designs (plate or cylinder)
477 suggest that the effect of flow velocity on the water boundary layer thickness calculated from
478 Eq.6 could be weakly influenced by the geometry of the passive samplers used. Considering
479 the complexity of hydrodynamic conditions near a passive sampler, and the different positions
480 of the passive sampler in the fluid, this approximation yields a simple model that will need to
481 be validated with further data including measurement of water flow velocities.

482 In Figure 5, we calculated R_s values for pesticides with SR rods at flow velocities recorded by
483 Rusina et al. [5]. At low flow velocity ($v = 0.14 \text{ cm s}^{-1}$), the estimated R_s values for WBL
484 controlled pesticides ($\log K_{sw} > 2.7$) were lower by a mean factor of 10 than those
485 experimentally determined at 5 cm s^{-1} , and the change in transport mechanism occurred at \log
486 K_{sw} around 2.7 instead of 3.3. These extrapolated data could be used to calculate time-

487 weighted average concentrations of pesticides in freshwaters with only a representative field
488 measurement of water flow velocity. Another way to calculate δ_w could be to use an
489 adaptation of the PRCs model with deuterated PAHs or PCBs as described by Booij et al.
490 [36].

491 5 Conclusion

492 The calibration data for SR rods, R_s and K_{sw} were determined for 23 pesticides and 13
493 candidate PRCs in a laboratory calibration system over 14 d at two flow velocities. The
494 results show that an in situ exposure duration of 7 d kept the SR rod passive sampler
495 configuration in the linear or curvilinear uptake period for 19 pesticides. A change in transport
496 mechanism from polymer control to WBL control was observed for a log K_{sw} of around 3.3.
497 The isotropic exchange of candidate PRCs was demonstrated for 5 PRCs at 5 cm s⁻¹.
498 However, the influence of water flow velocity on elimination was not demonstrated. Hence,
499 the use of these PRCs was not validated to correct R_s for pesticides with WBL-controlled
500 uptake kinetics.

501 Considering the PRC results, we propose an alternative method based on the overall
502 resistance to mass transfer model to adjust R_s from laboratory experiments to other
503 hydrodynamic conditions by measuring in situ flow velocities. The theoretical model of
504 overall resistance to mass transfer was applied to our experimental data using log D_s values
505 and δ_w as adjustable parameters. The estimated log D_s values ranging from -12.13 to -10.07
506 m² s⁻¹ for pesticides were consistent with values previously determined for PAHs and PCBs.
507 Nonetheless, the application of a two-phase Fickian model could lead to more accurate
508 results; for this purpose, calibration results are detailed in an additional spreadsheet (SI-7).
509 Moreover, we demonstrated a power function correlation between δ_w and water velocity using
510 a compilation of data from the present study and from Rusina et al. [5]. This correlation is

511 apparently not influenced by passive sampler geometry. Thus, the estimation of new R_s
512 requires only direct measurements of flow velocity in the deployment location of the SR-
513 based passive sampler. Considering isotropic exchanges, δ_w values could also be estimated
514 with WBL-controlled PRCs (PAHs, PCBs). However, further experiments are required to
515 address isotropic exchange and significant dissipation of PRCs with the SR rod configuration.

516 6 Acknowledgments

517 The authors thank Claire Lauvernet (Irstea) for help in R script programming and Matthieu
518 Masson's team (Irstea) for analysis of water. This work was funded by the French Agency for
519 Biodiversity (AFB) and the French National Research Agency (ANR) through the PoToMAC
520 project (ANR 2011 CESA 022 02). We thank ATT for English language editing. The authors
521 declare no conflict of interest.

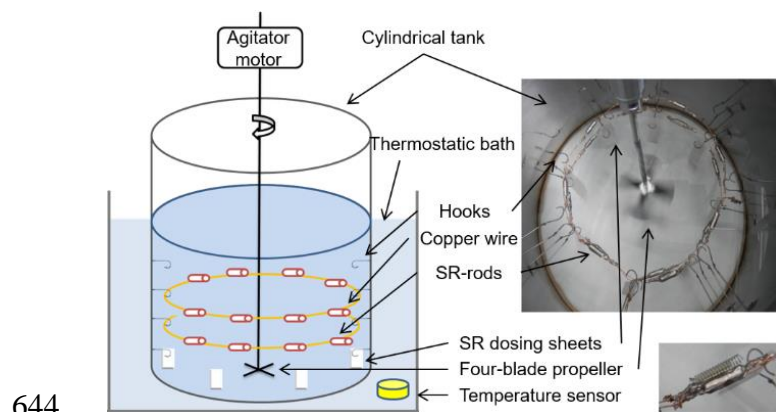
522 7 References

- 523 1. Rabiet M, Margoum C, Gouy V, Carluer N, Coquery M. 2010. Assessing pesticide
524 concentrations and fluxes in the stream of a small vineyard catchment-effect of
525 sampling frequency. *Environ. Pollut.* 158:737-748.
- 526 2. Poulhier G, Lissalde S, Charriau A, Buzier R, Delmas F, Gery K, Moreira A, Guibaud
527 G, Mazzella N. 2014. Can POCIS be used in Water Framework Directive
528 (2000/60/EC) monitoring networks? A study focusing on pesticides in a French
529 agricultural watershed. *Sci. Total Environ.* 497-498:282-292.
- 530 3. Miège C, Mazzella N, Allan I, Dulio V, Smedes F, Tixier C, Vermeirssen E, Brant J,
531 O'Toole S, Budzinski H, Ghestem J-P, Staub P-F, Lardy-Fontan S, Gonzalez J-L,
532 Coquery M, Vrana B. 2015. Position paper on passive sampling techniques for the
533 monitoring of contaminants in the aquatic environment – Achievements to date and
534 perspectives. *Trends Anal. Chem.* 8:20-26.
- 535 4. Assoumani A, Margoum C, Chataing S, Guillemain C, Coquery M. 2014. Use of
536 passive stir bar sorptive extraction as a simple integrative sampling technique of
537 pesticides in freshwaters: determination of sampling rates and lag-phases. *J.*
538 *Chromatogr. A.* 1333:1-8.
- 539 5. Rusina TP, Smedes F, Koblizkova M, Klanova J. 2010. Calibration of Silicone Rubber
540 Passive Samplers: Experimental and Modeled Relations between Sampling Rate and
541 Compound Properties. *Environ. Sci. Technol.* 44:362-367.
- 542 6. Vrana B, Komancova L, Sobotka J. 2016. Calibration of a passive sampler based on
543 stir bar sorptive extraction for the monitoring of hydrophobic organic pollutants in
544 water. *Talanta.* 152:90-97.

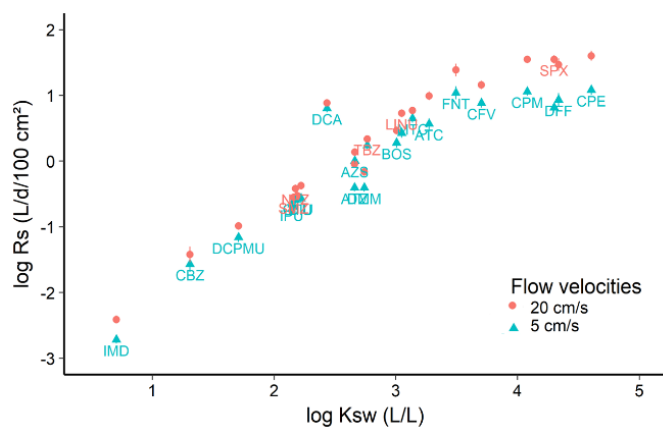
- 545 7. Estoppey N, Schopfer A, Omlin J, Esseiva P, Vermeirssen ELM, Delémont O, De
546 Alencastro LF. 2014. Effect of water velocity on the uptake of polychlorinated
547 biphenyls (PCBs) by silicone rubber (SR) and low-density polyethylene (LDPE)
548 passive samplers: An assessment of the efficiency of performance reference
549 compounds (PRCs) in river-like flow conditions. *Sci. Total Environ.* 499:319-326.
- 550 8. Estoppey N, Schopfer A, Fong C, Delemont O, De Alencastro LF, Esseiva P. 2016.
551 An in-situ assessment of low-density polyethylene and silicone rubber passive
552 samplers using methods with and without performance reference compounds in the
553 context of investigation of polychlorinated biphenyl sources in rivers. *Sci. Total*
554 *Environ.* 572:794-803.
- 555 9. Belles A, Alary C, Mamindy-Pajany Y. 2016. Thickness and material selection of
556 polymeric passive samplers for polycyclic aromatic hydrocarbons in water: Which
557 more strongly affects sampler properties? *Environ. Toxicol. Chem.* 35:1708-1717.
- 558 10. Jacquet R, Miege C, Smedes F, Tixier C, Tronczynski J, Togola A, Berho C, Valor I,
559 Llorca J, Barillon B, Marchand P, Coquery M. 2014. Comparison of five integrative
560 samplers in laboratory for the monitoring of indicator and dioxin-like polychlorinated
561 biphenyls in water. *Chemosphere.* 98:18-27.
- 562 11. Allan IJ, Booij K, Paschke A, Vrana B, Mills GA, Greenwood R. 2010. Short-term
563 exposure testing of six different passive samplers for the monitoring of hydrophobic
564 contaminants in water. *J. Environ. Monit.* 12:696-703.
- 565 12. Schellin M, Popp P. 2007. Application of a polysiloxane-based extraction method
566 combined with large volume injection-gas chromatography-mass spectrometry of
567 organic compounds in water samples. *J. Chromatogr. A.* 1152:175-183.
- 568 13. Martin A, Margoum C, Randon J, Coquery M. 2016. Silicone rubber selection for
569 passive sampling of pesticides in water. *Talanta.* 160:306-313.
- 570 14. Heltsley RM. 2004. Novel methods for monitoring chlorinated contaminants in
571 aquatic environments. PhD thesis. Department of environmental and molecular
572 toxicology. North Carolina State University, US.
- 573 15. Kwon JH, Wuethrich T, Mayer P, Escher BI. 2007. Dynamic permeation method to
574 determine partition coefficients of highly hydrophobic chemicals between
575 poly(dimethylsiloxane) and water. *Anal. Chem.* 79:6816-6822.
- 576 16. Magner JA, Alsberg TE, Broman D. 2009. Evaluation of poly(ethylene-co-ninyl
577 acetate-co-carbon monoxide) and polydimethylsiloxane for equilibrium sampling of
578 polar organic contaminants in water. *Environ. Toxicol. Chem.* 28:1874-1880.
- 579 17. Ahrens L, Daneshvar A, Lau AE, Kreuger J. 2015. Characterization of five passive
580 sampling devices for monitoring of pesticides in water. *J. Chromatogr. A.* 1405:1-11.
- 581 18. Narvaez Valderrama JF, Baek K, Molina FJ, Allan IJ. 2016. Implications of observed
582 PBDE diffusion coefficients in low density polyethylene and silicone rubber. *Environ.*
583 *Sci.: Processes Impacts.* 18:87-94.
- 584 19. Pintado-Herrera MG, Lara-Martin PA, Gonzalez-Mazo E, Allan IJ. 2016.
585 Determination of silicone rubber and low-density polyethylene diffusion and
586 polymer/water partition coefficients for emerging contaminants. *Environ. Toxicol.*
587 *Chem.* 35:2162-2172.
- 588 20. Rusina TP, Smedes F, Klanova J. 2010. Diffusion Coefficients of Polychlorinated
589 Biphenyls and Polycyclic Aromatic Hydrocarbons in Polydimethylsiloxane and Low-
590 Density Polyethylene Polymers. *J. Appl. Polym. Sci.* 116:1803-1810.
- 591 21. Jonker MTO, van der Heijden SA, Kotte M, Smedes F. 2015. Quantifying the Effects
592 of Temperature and Salinity on Partitioning of Hydrophobic Organic Chemicals to
593 Silicone Rubber Passive Samplers. *Environ. Sci. Technol.* 49:6791-6799.

- 594 22. Booij K, van Bommel R, Mets A, Dekker R. 2006. Little effect of excessive
595 biofouling on the uptake of organic contaminants by semipermeable membrane
596 devices. *Chemosphere*. 65:2485-2492.
- 597 23. Allan IJ, Harman C, Kringstad A, Bratsberg E. 2010. Effect of sampler material on the
598 uptake of PAHs into passive sampling devices. *Chemosphere*. 79:470-475.
- 599 24. Booij K Smedes F. 2010. An Improved Method for Estimating in Situ Sampling Rates
600 of Nonpolar Passive Samplers. *Environ. Sci. Technol.* 44:6789-6794.
- 601 25. O'Brien D, Komarova T, Mueller JF. 2012. Determination of deployment specific
602 chemical uptake rates for SPMD and PDMS using a passive flow monitor. *Mar.*
603 *Pollut. Bull.* 64:1005-1011.
- 604 26. Greenwood R, Mills G, Vrana B. 2007. *Passive Sampling Techniques in*
605 *Environmental Monitoring*, 1st Edition. Elsevier, Amsterdam, The Netherlands.
- 606 27. Emelogu ES, Pollard P, Robinson CD, Webster L, McKenzie C, Napier F, Steven L,
607 Moffat CF. 2013. Identification of selected organic contaminants in streams associated
608 with agricultural activities and comparison between autosampling and silicone rubber
609 passive sampling. *Sci. Total Environ.* 445:261-272.
- 610 28. Huckins JN, Petty JD, Booij K. 2006. *Monitors of Organic Chemicals in the*
611 *Environment. Semipermeable Membrane Devices*. Springer, New York NY, USA.
- 612 29. Tcaciuc AP, Apell JN, Gschwend PM. 2015. Modeling the transport of organic
613 chemicals between polyethylene passive samplers and water in finite and infinite bath
614 conditions. *Environ. Toxicol. Chem.* 34:2739-2749.
- 615 30. Allan IJ, Harman C, Ranneklev SB, Thomas KV, Grung M. 2013. Passive sampling
616 for target and nontarget analyses of moderately polar and nonpolar substances in
617 water. *Environ. Toxicol. Chem.* 32:1718-1726.
- 618 31. Zhao WN, Ouyang GF, Alae M, Pawliszyn J. 2006. On-rod standardization technique
619 for time-weighted average water sampling with a polydimethylsiloxane rod. *J.*
620 *Chromatogr. A.* 1124:112-120.
- 621 32. Rusina TP, Smedes F, Klanova J, Booij K, Holoubek I. 2007. Polymer selection for
622 passive sampling: a comparison of critical properties. *Chemosphere*. 68:1344-1351.
- 623 33. Allan IJ, Booij K, Paschke A, Vrana B, Mills GA, Greenwood R. 2009. Field
624 performance of seven passive sampling devices for monitoring of hydrophobic
625 substances. *Environ. Sci. Technol.* 43:5383-5390.
- 626 34. Morin N, Camilleri J, Cren-Olivé C, Coquery M, Miège C. 2013. Determination of
627 uptake kinetics and sampling rates for 56 organic micropollutants using
628 "pharmaceutical" POCIS. *Talanta*. 109:61-73.
- 629 35. Thompson JM, Hsieh C-H, Luthy RG. 2015. Modeling uptake of hydrophobic organic
630 contaminants into polyethylene passive samplers. *Environ. Sci. Technol.* 49:2270-
631 2277.
- 632 36. Booij K, Smedes F, van Weerlee EM. 2002. Spiking of performance reference
633 compounds in low density polyethylene and silicone passive water samplers.
634 *Chemosphere*. 46:1157-1161.
- 635 37. Hayduk W, Laudie H. 1974. Prediction of diffusion coefficients for nonelectrolytes in
636 dilute aqueous solutions. *AIChE Journal*. 20:611-615.
- 637 38. ter Laak TL, Busser FJ, Hermens JL. 2008. Poly(dimethylsiloxane) as passive sampler
638 material for hydrophobic chemicals: effect of chemical properties and sampler
639 characteristics on partitioning and equilibration times. *Anal. Chem.* 80:3859-3866.
- 640

641 Figure 1. Schematic diagram of the laboratory static calibration system (a), depiction of the
642 inside of the calibration tank with the SR rods (b) and zoom on SR-rods inserted in a spring
643 (c)



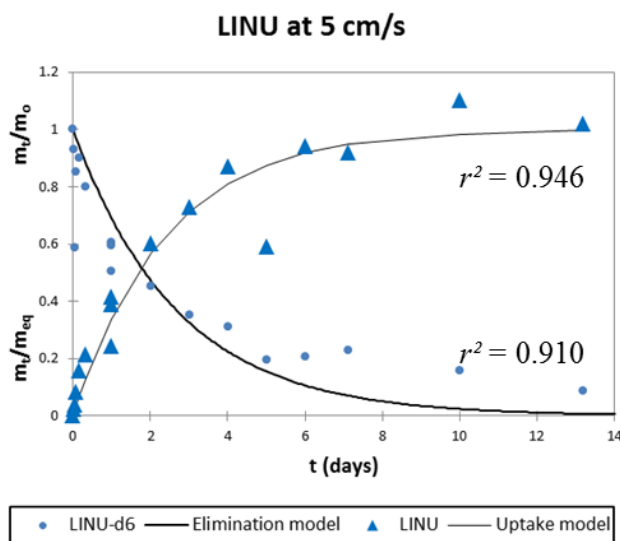
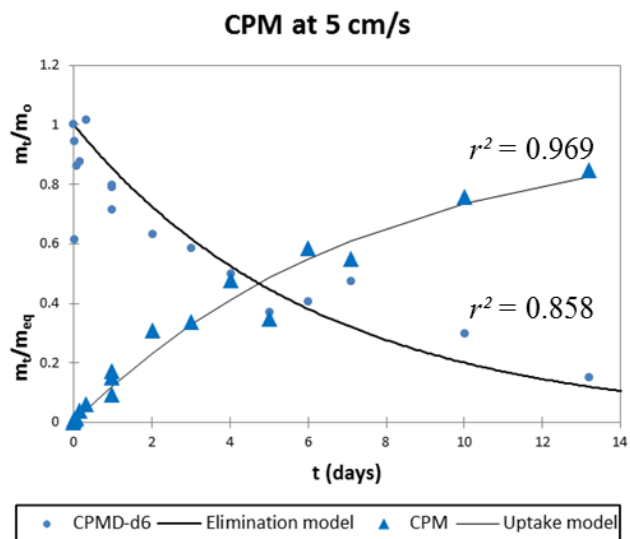
646 Figure 2. Plot of $\log R_s$ normalised per 100 cm² versus $\log K_{sw}$ in our experiment at two flow
647 velocities. Error is expressed as standard deviation.



648

649

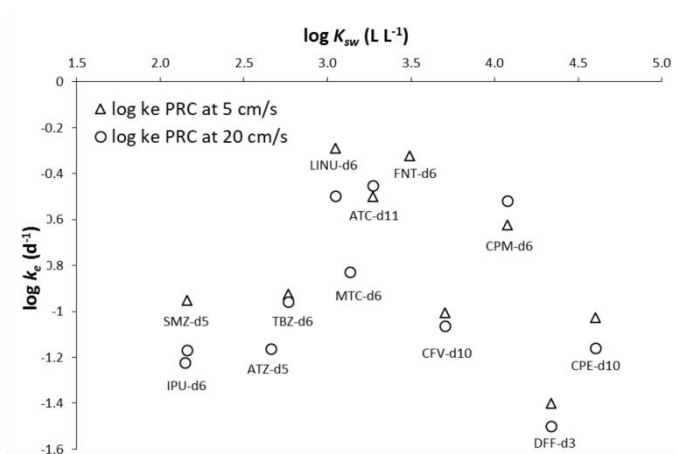
650 Figure 3. The uptake of CPM and LINU and release of corresponding deuterated pesticides
651 (CPM-d6 and LINU-d6) by SR rods. Mass ratios are plotted relative to the initial mass for the
652 release (m_0) and to the predicted equilibrium mass for the uptake (m_{eq}) with triangles for 5 cm
653 s^{-1} and circles for 20 $cm s^{-1}$.



654

655

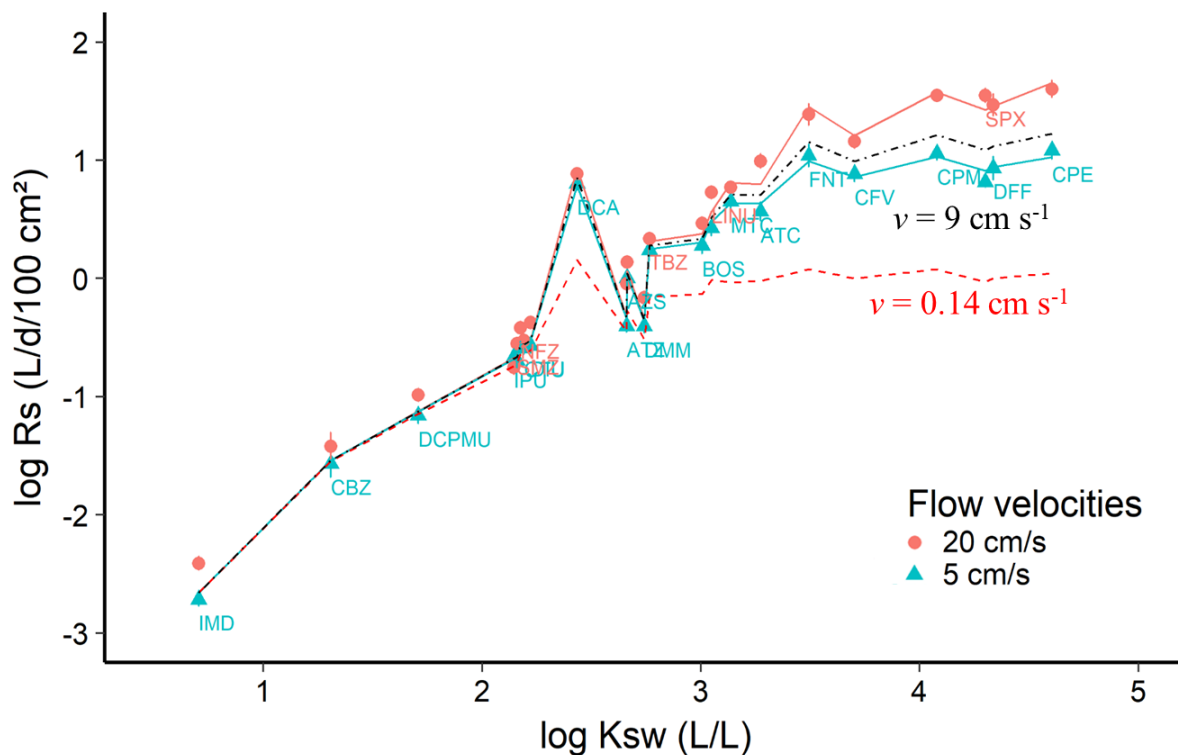
656 Figure 4. Plot of $\log k_e PRC$ versus $\log K_{sw}$ in experiments at two flow velocities (5 and 20 cm
657 s^{-1}).



658

659

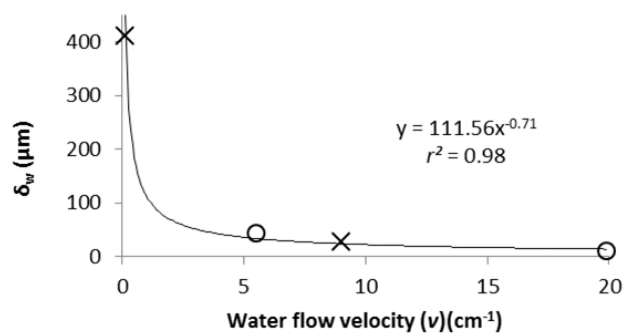
660 Figure 5. Plot of $\log R_s$ normalised per 100 cm^2 versus $\log K_{sw}$ in experiments at two flow
661 velocities (5 and 20 cm s^{-1}) with theoretical model (solid lines) and estimated by theoretical
662 model (dotted lines) for other flow velocities (0.14 and 9 cm s^{-1} with data from Rusina et al.
663 [5]).



664

665

666 Figure 6. Plot of water boundary layer thickness (δ_w) estimated by theoretical model (Eq. 6)
667 versus water flow velocity (v) from this present study (circles) and Rusina et al. [5] (crosses).



668

669 **Table 1. Physico-chemical properties, kinetic parameters at two flow velocities and estimated diffusion coefficients of the**
 670 **studied pesticides.**

Pesticide name	Abbreviation	Log K_{ow} ^a	Water concentration	Solvent back	Log K_{sw}	Log K_{sw}	R_s	R_s	$t_{1/2}$	$t_{1/2}$	Log D_s
			($\mu\text{g L}^{-1}$)	extraction	(L L^{-1})	(L L^{-1})	(mL d^{-1})	(mL d^{-1})	(d)	(d)	($\text{m}^2 \text{s}^{-1}$)
			Mean value	Mean value	5 cm s^{-1}	20 cm s^{-1}	5 cm s^{-1}	20 cm s^{-1}	5 cm s^{-1}	20 cm s^{-1}	Estimated
			$n = 30$, RSD (%)	$n = 3$, sd.	$n = 20$, sd.	$n = 20$, sd.	$n = 20$, RSD (%)	$n = 20$, RSD (%)			values
Acetochlor	ATC	4.1	2.8 (13)	69 (9)	3.18 (0.03)	3.27 (0.01)	75 (19)	200 (14)	2.3	0.9	-11.17
Atrazine	ATZ	2.7	1.5 (24)	86 (4)	2.47 (0.04)	2.66 (0.02)	8.0 (12)	18 (8)	5.3	2.3	-11.75
Azoxystrobin	AZS	2.5	1.2 (15)	95 (6)	2.87 (0.03)	2.66 (0.02)	20 (10)	28 (10)	2.1	1.5	-11.35
Boscalid	BOS	3.0	1.8 (16)	80 (7)	2.89 (0.03)	3.01 (0.02)	38 (16)	59 (12)	2.4	1.6	-11.36
Carbendazim	CBZ	1.5	0.4 (16)	82 (21)	1.41 (0.04)	1.31 (0.03)	0.5 (27)	0.8 (27)	3.4	2.4	-11.61
Chlorfenvinphos	CFV	3.8	2.7 (9)	82 (10)	3.82 (0.04)	3.70 (0.01)	155 (16)	293 (14)	3	1.6	-11.05
Chlorpyrifos-ethyl	CPE	4.7	1.6 (14)	60 (10)	-	4.60 (0.03)	245 (17)	812 (17)	15.2	4.6	-10.07
Chlorpyrifos-methyl	CPM	4	1.9 (12)	68 (6)	4.12 (0.05)	4.08 (0.01)	231 (13)	714 (10)	4.8	1.5	-10.67
Chlortoluron	CTU	2.5	1.8 (11)	90 (9)	1.76 (0.02)	2.19 (0.01)	5.5 (17)	6.1 (12)	2.6	2.4	-11.50
3,4-dichloroaniline	DCA	2.7	0.9 (20)	87 (6)	2.19 (0.01)	2.43 (0.01)	129 (13)	156 (11)	0.2	0.2	-10.20
3-(3,4-dichlorophenyl)- 1-methylurea	DCPMU	2.9*	1.5 (19)	91 (10)	1.53 (0.03)	1.71 (0.02)	1.4 (16)	2.1 (13)	3.4	2.2	-11.59
Diflufenican	DFE	4.2	1.4 (15)	69 (15)	4.37 (0.14)	4.34 (0.02)	174 (24)	598 (22)	11.5	3.3	-11.15
Diuron	DIU	2.9	2.0 (12)	87 (8)	2.13 (0.03)	2.22 (0.02)	5.5 (16)	8.6 (13)	2.8	1.8	-11.50
Dimethomorph	DMM	2.7	1.8 (16)	96 (12)	2.81 (0.04)	2.74 (0.02)	8.0 (14)	14 (14)	6.4	3.7	-11.84
Fenitrothion	FNT	3.3	24.1 (15)	76 (13)	3.37 (0.02)	3.49 (0.01)	222 (22)	495 (21)	1.3	0.6	-10.45
Imidacloprid	IMD	0.6	1.1 (8)	91 (11)	0.42 (0.04)	0.71 (0.04)	0.04 (13)	0.08 (13)	12	5.9	-12.13
Isoproturon	IPU	2.5	1.8 (11)	96 (12)	2.22 (0.03)	2.15 (0.02)	4.4 (16)	3.6 (13)	2.9	3.6	-11.58
Linuron	LINU	3.0	3.1 (13)	73 (6)	2.99 (0.03)	3.05 (0.01)	54 (16)	109 (13)	1.9	0.9	-11.21
Metolachlor	MTC	3.4	2.2 (10)	75 (5)	3.17 (0.02)	3.14 (0.01)	91 (14)	120 (10)	1.4	1.1	-11.02
Norflurazon	NFZ	2.5	1.9 (17)	98 (8)	2.04 (0.02)	2.18 (0.02)	5.2 (13)	7.8 (12)	2.6	1.8	-11.48
Procymidone	PCM	3.3	9.6 (41)	69 (19)	-	-	-	-			-
Simazine	SMZ	2.3	1.5 (21)	97 (8)	2.09 (0.03)	2.16 (0.02)	4.1 (14)	5.7 (11)	3.2	2.3	-11.58
Spiroxamine	SPX	5.5*	0.5 (27)	88 (9)	-	4.30 (0.03)	133 (11)	717 (14)	13.9	2.6	-11.15
Tebuconazole	TBZ	3.7	23.9 (15)	87 (6)	2.95 (0.03)	2.77 (0.01)	35 (12)	44 (10)	1.5	1.2	-11.19

671 ^a University of Hertfordshire. Pesticide Properties DataBase: <http://sitem.herts.ac.uk/aeru/ppdb/en/atoz.htm>

672 * Predicted by ChemAxon: <http://www.chemicalize.org/structure>

Calibration of silicone rubber rods as passive samplers for pesticides at two different flow velocities: Modelling of sampling rates under water boundary layer and polymer control

A. Martin †, C. Margoum* †, A. Jolivet †, A. Assoumani †, B. El Moujahid †, J. Randon ‡, M. Coquery †

† Irstea, UR MALY, 5 rue de la Doua, BP 32108, F-69616 Villeurbanne Cedex, France

‡ Univ Lyon, CNRS, Université Claude Bernard Lyon 1, ENS de Lyon, Institut des Sciences Analytiques, UMR 5280, 5 rue de la Doua, F-69100 Villeurbanne, France

*Corresponding author: Tel: + 33 4 72 20 87 11; Fax: + 33 4 78 47 78 75; Email address: christelle.margoum@irstea.fr

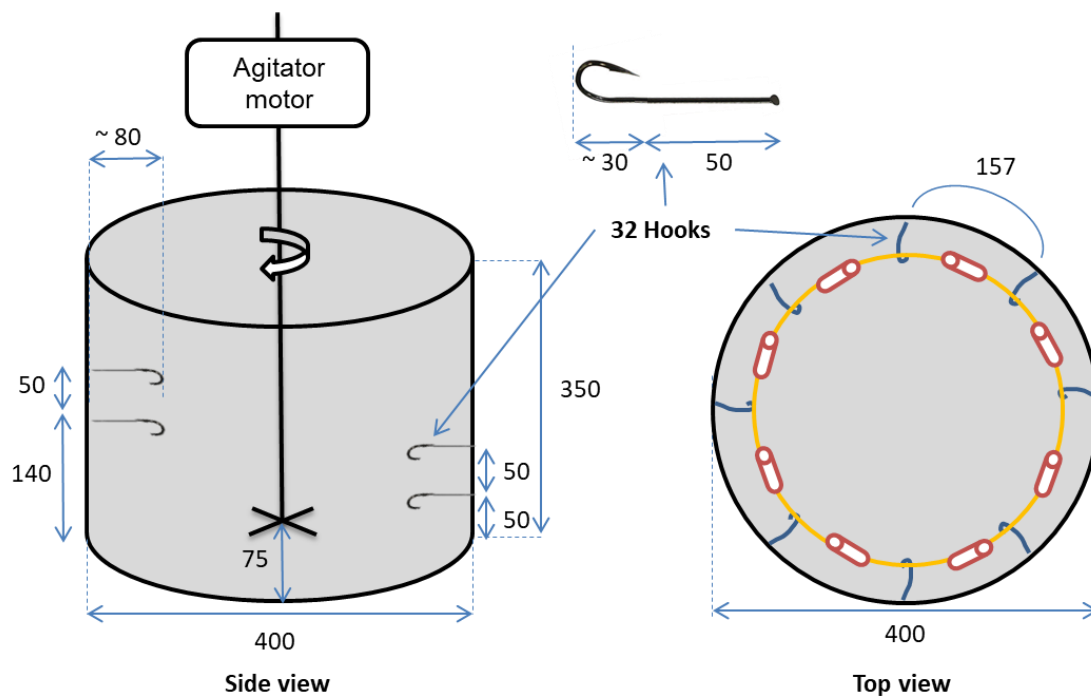
Supplementary Information

SI-1. Pesticide parameters for UHPLC-MS/MS analysis.

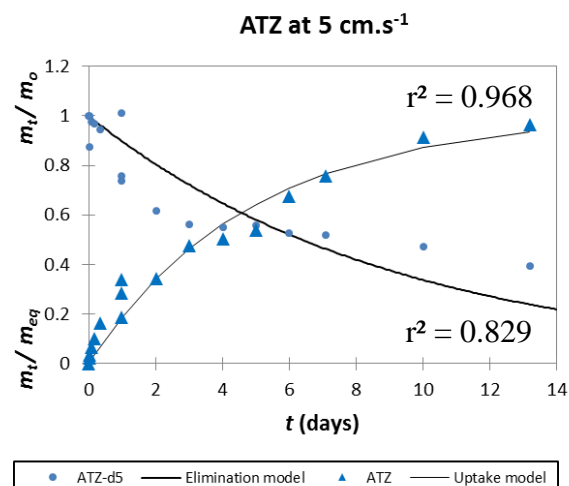
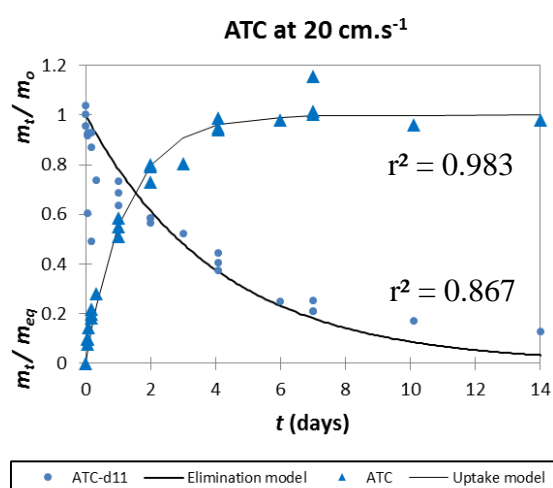
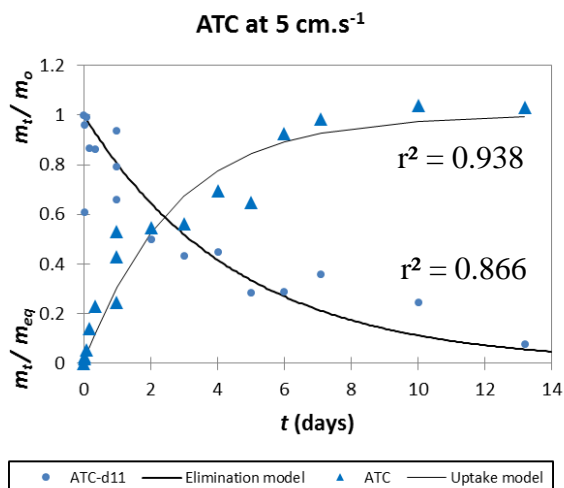
Compound	LOQ ($\mu\text{g L}^{-1}$)	Quantification transitions (m/z)	Declustering potential (V)	Collision energy (V)	Collision exit potential (V)
ATC	0.40	269.9 > 224.2 ;	31	15	16
		269.9 > 148.1	31	27	14
ATZ	0.10	215.9 > 174.1 ;	66	25	16
		215.9 > 104.1	66	41	8
AZS	0.02	404 > 372 ;	61	33	26
		404 > 344	61	35	28
BOS	0.20	343 > 307 ;	81	25	28
		343 > 140	81	29	8
CBZ	0.02	192 > 160 ;	56	25	16
		192 > 132	56	41	24
CFV	0.16	359 > 155 ;	76	17	20
		359 > 99	76	43	8
CPE	0.40	352 > 200 ;	45	30	38
		350 > 97	61	55	4
CPM	0.40	322 > 125 ;	71	29	22
		322 > 290	71	23	54
CTU	0.40	213 > 72 ;	51	25	12
		213 > 140	51	37	6
DCA	0.40	162 > 127 ;	51	31	24
		162 > 74	51	73	14
DCPMU	0.16	219 > 162 ;	66	21	26
		219 > 127	66	37	22
DFE	0.40	395 > 266 ;	86	35	28
		395 > 246	86	47	40
DIU	0.40	233 > 72 ;	46	51	6
		233 > 46	46	37	8
DMM	0.16	388 > 301 ;	76	31	36
		388 > 165	76	43	28
FNT	4.00	278 > 125 ;	71	29	22
		278 > 109	71	25	16
IMD	0.10	256 > 209.1 ;	61	23	38
		256 > 175.1	61	27	12
IPU	0.16	207 > 72 ;	51	37	8
		207 > 165	51	19	28
LINU	0.16	249 > 160 ;	61	25	32
		249 > 182	61	19	12
MTC	0.04	284.1 > 252.2 ;	46	21	20
		284.1 > 176.2	46	37	4
NFZ	0.40	304 > 284 ;	101	35	26
		304 > 88	101	61	16
PCM	1.60	284 > 256	76	25	46
SMZ	0.02	202.1 > 132.2 ;	56	29	10
		202.1 > 124.1	56	27	10
SPX	0.16	298 > 144 ;	51	31	8
		298 > 100	51	45	18
TBZ	0.16	308 > 70 ;	76	51	12
		308 > 125	76	57	12

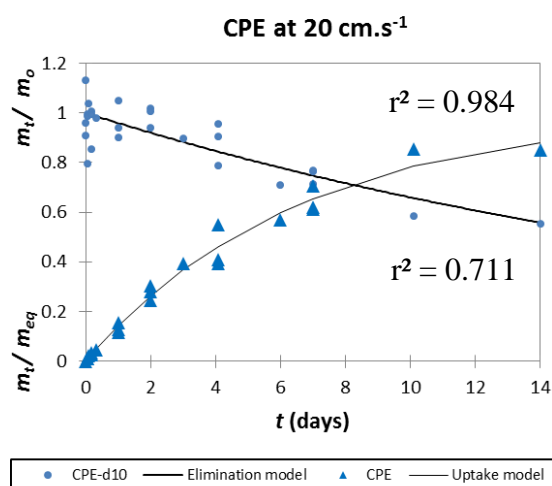
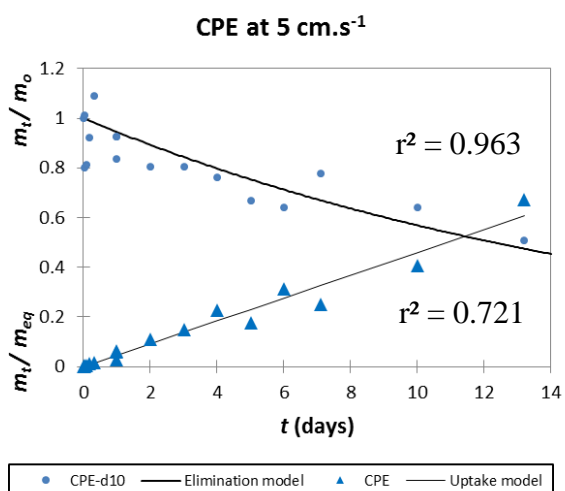
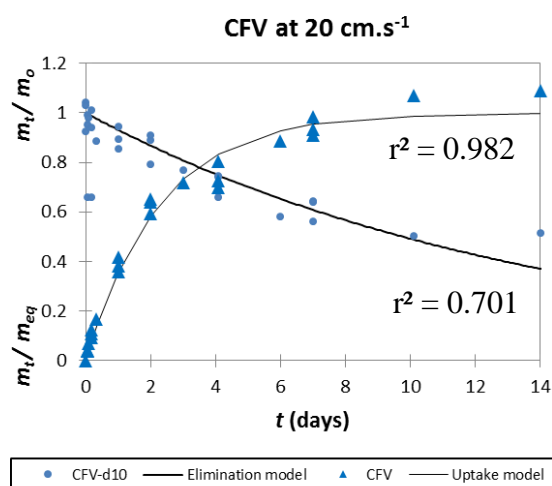
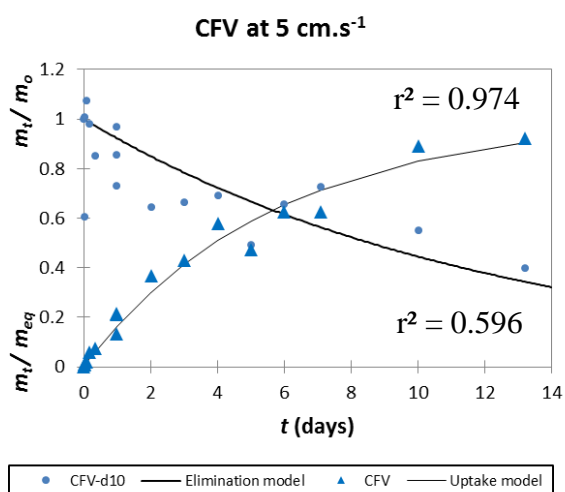
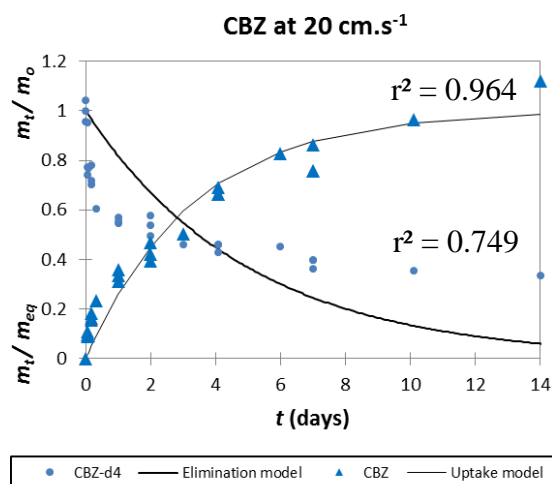
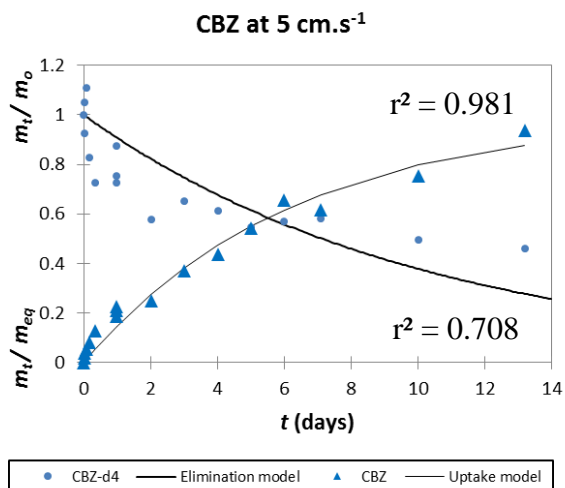
Compound	LOQ ($\mu\text{g L}^{-1}$)	Quantification transitions (m/z)	Declustering potential (V)	Collision energy (V)	Collision exit potential (V)
ATC-d11	0.40	281.1 > 235.1 ;	31	13	20
		281.1 > 159.1	31	29	12
ATZ-d5	0.10	221.06 > 179.1 ;	46	27	18
		221.06 > 101.1	46	35	18
CBZ-d4	0.02	196 > 164.1 ;	61	29	12
		196 > 138.1	61	41	8
CFV-d10	0.16	369.1 > 165.2 ;	56	19	10
		369.1 > 101.2	56	45	10
CPE-d10	0.40	360 > 199 ;	66	29	14
		360 > 163	66	21	14
CPM-d6	0.40	328 > 131.2 ;	66	31	8
		328 > 292.9	66	23	22
DFP-d3	0.40	398 > 268 ;	76	31	16
		398 > 248	76	49	20
DIU d6	0.40	239 > 78 ;	66	43	14
		239 > 52	66	37	10
FNT-d6	4.00	284 > 131 ;	61	27	18
		284 > 249	61	25	12
IPU-d6	0.16	213.1 > 78.3 ;	66	27	24
		213.1 > 171.2	66	21	10
LINU-d6	0.16	255 > 159.9 ;	56	25	8
		255 > 185	56	21	14
MTC-d6	0.04	290.1 > 258.1 ;	65	21	22
		290.1 > 182.2	65	35	32
SMZ-d5	0.02	207 > 129.1 ;	71	29	6
		207 > 137.1	71	27	8
TBZ-d6	0.16	314 > 72 ;	81	77	12
		314 > 125	81	53	10

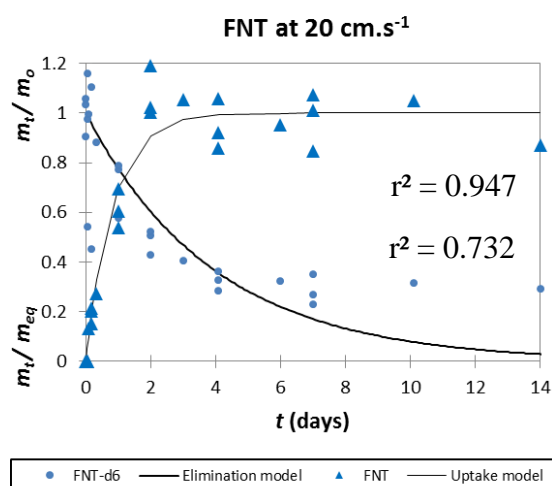
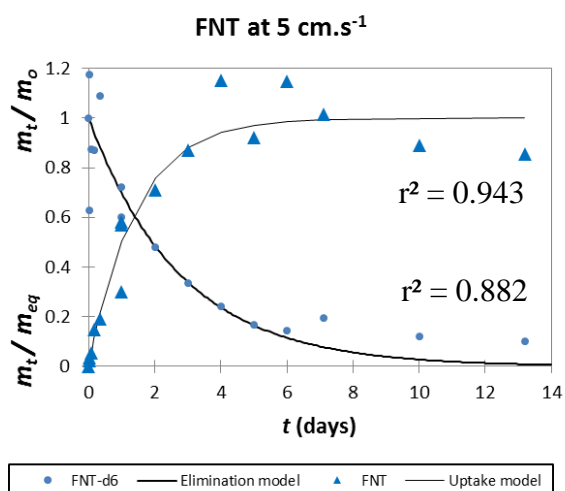
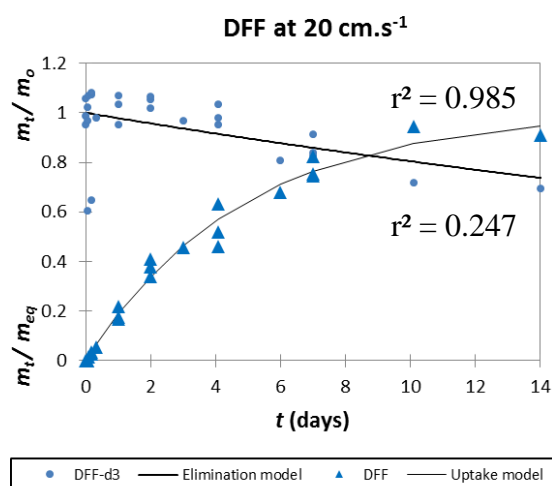
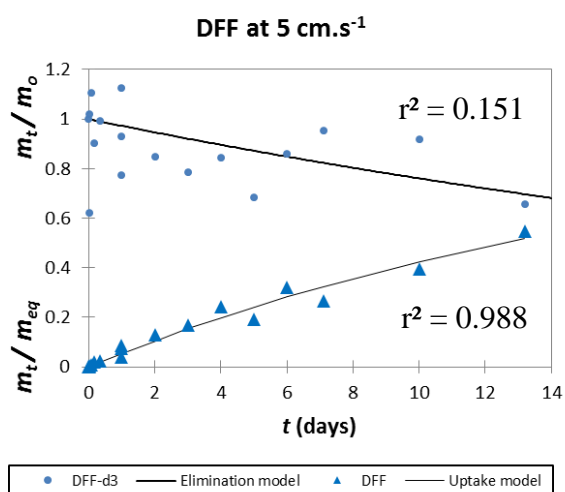
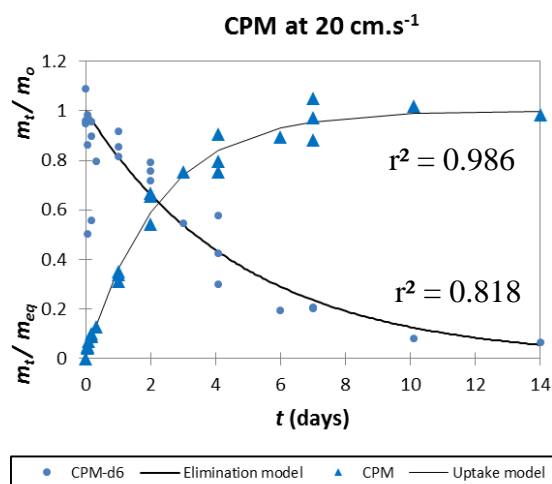
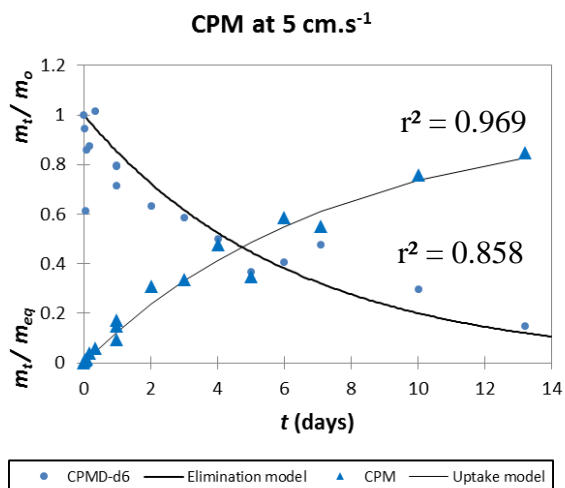
SI-2. Schematic diagrams (top and side view) of the laboratory static calibration system with dimensions in mm.

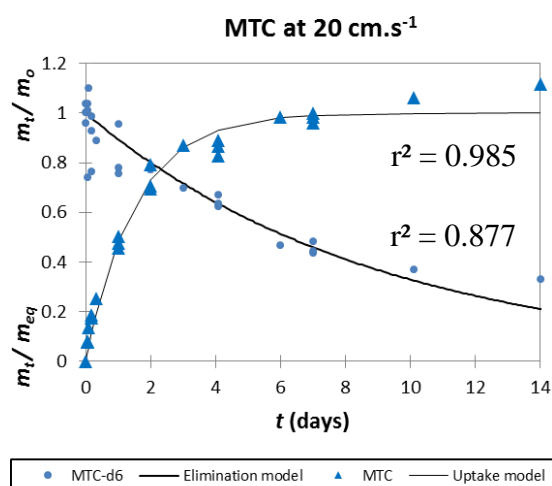
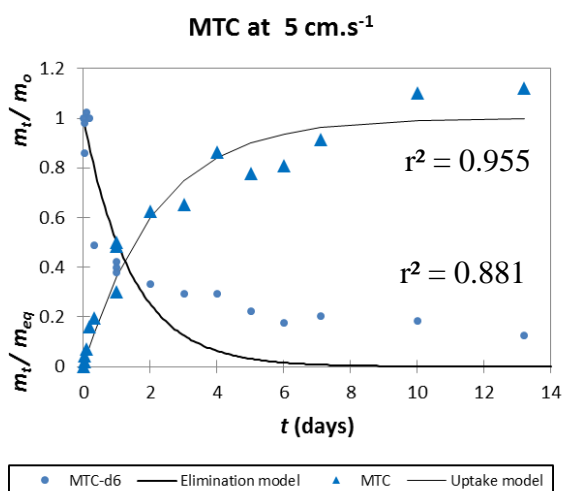
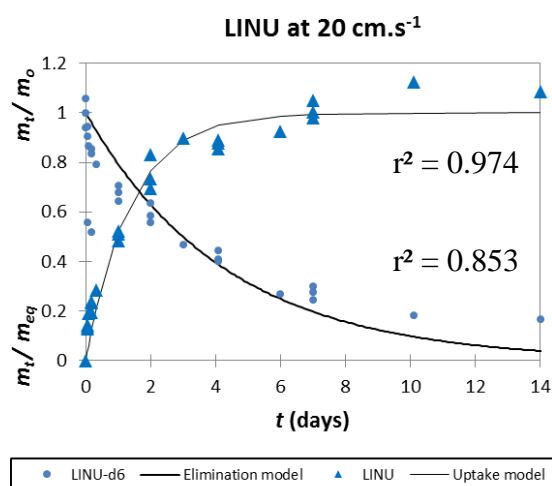
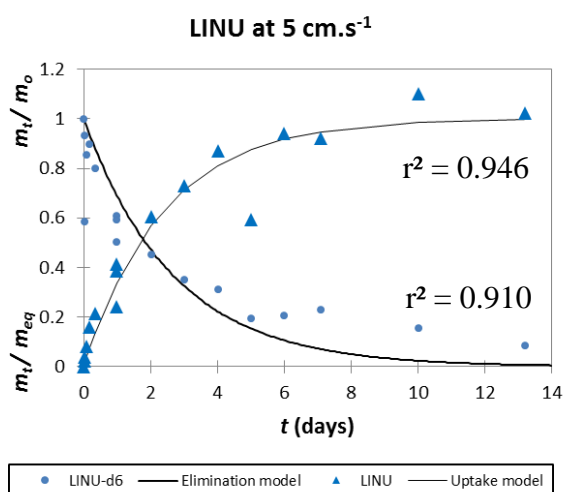
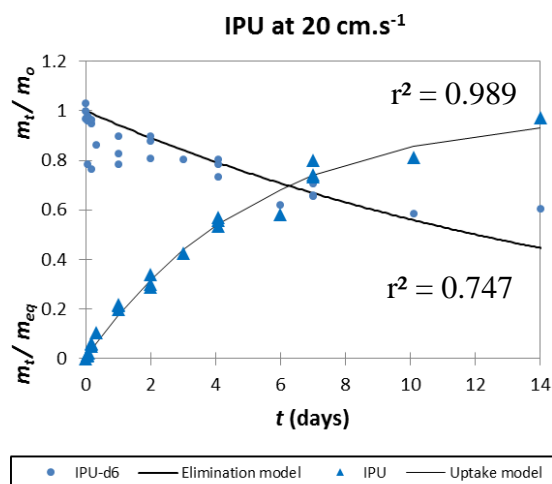
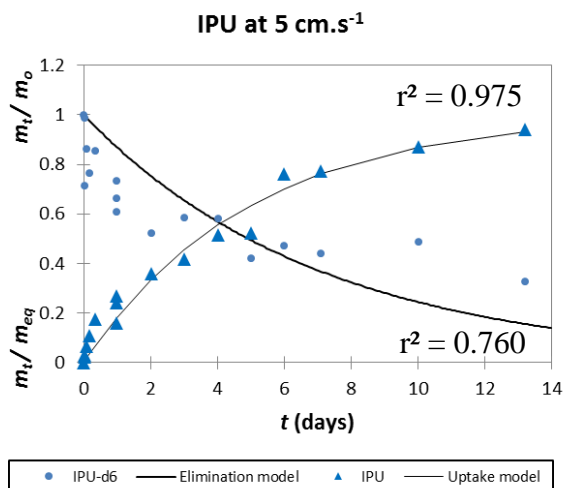


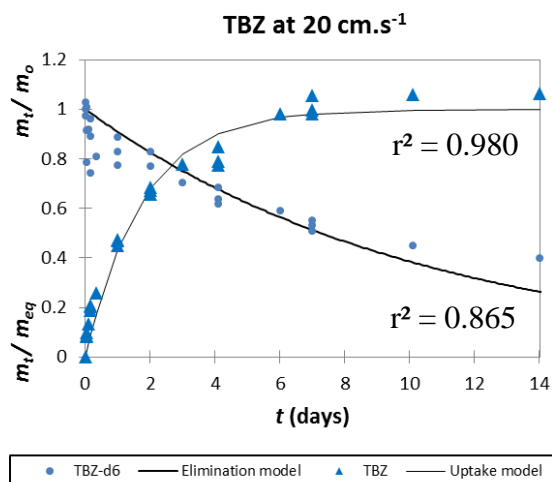
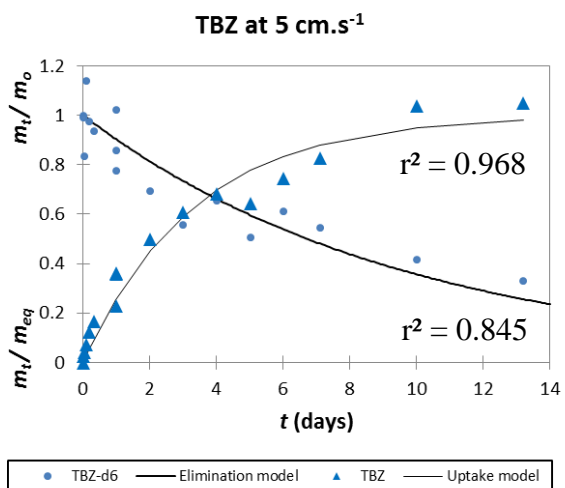
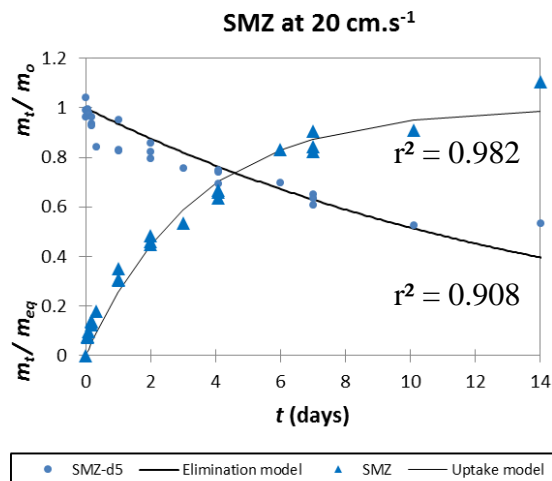
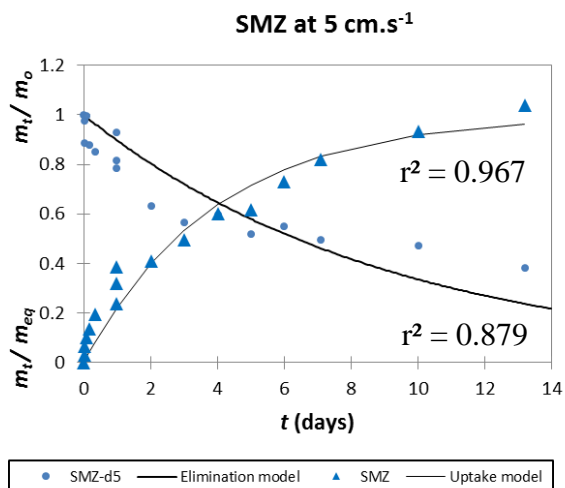
SI-3. Uptake of pesticides and release of corresponding deuterated pesticide
(candidate PRCs) by the silicone rods (SRs) at two flow velocities (5 and 20 $\text{cm}\cdot\text{s}^{-1}$).
Accumulated mass (m) is plotted relative to the initial mass for the release (m_0) and to the predicted equilibrium mass for the uptake (m_{eq}).



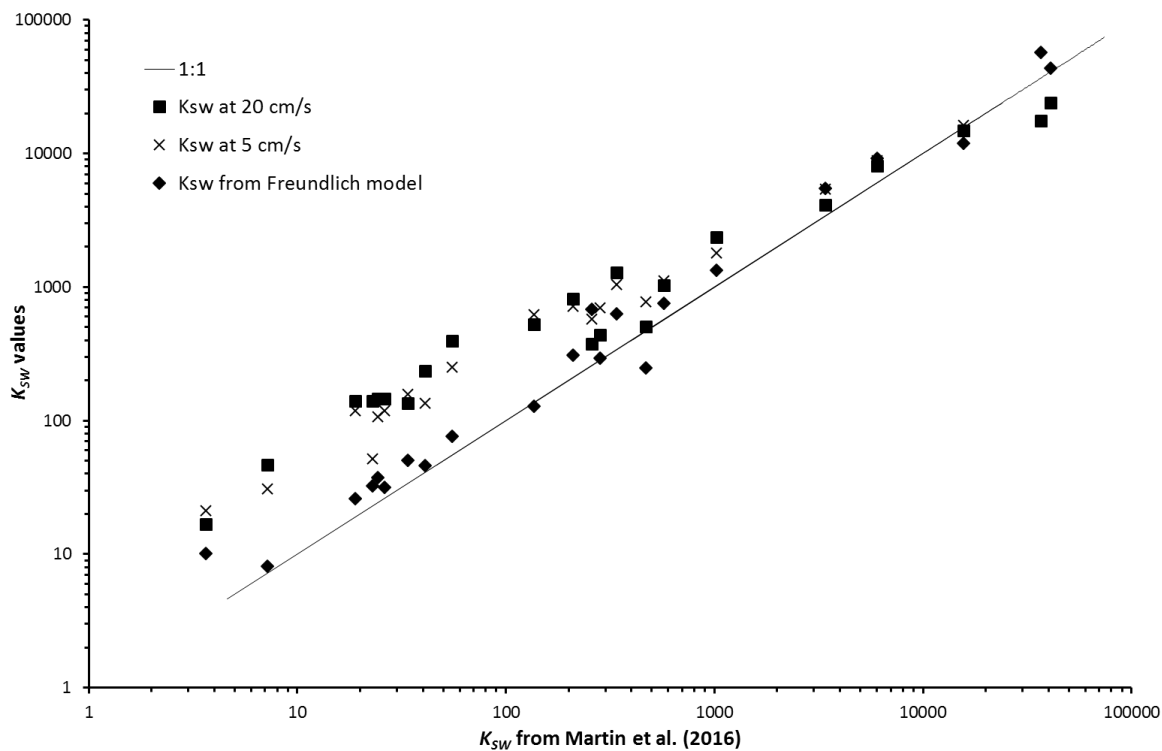








SI-4. Plot of K_{sw} values from the experiments at two flow velocities (Eq.7) and estimated by the Freundlich model ($K_{sw} = K_f C_w eq^{1/n-1}$ with parameters from Martin et al. [1]) at the concentration of this experiment against K_{sw} estimated in Martin et al. [1].



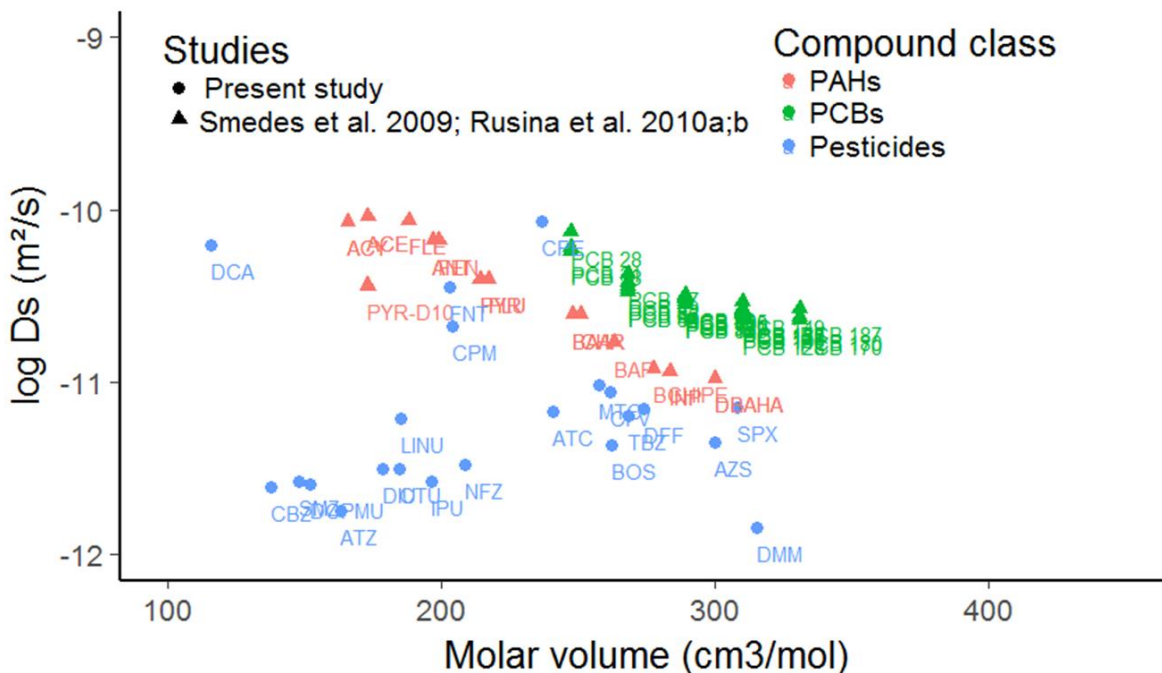
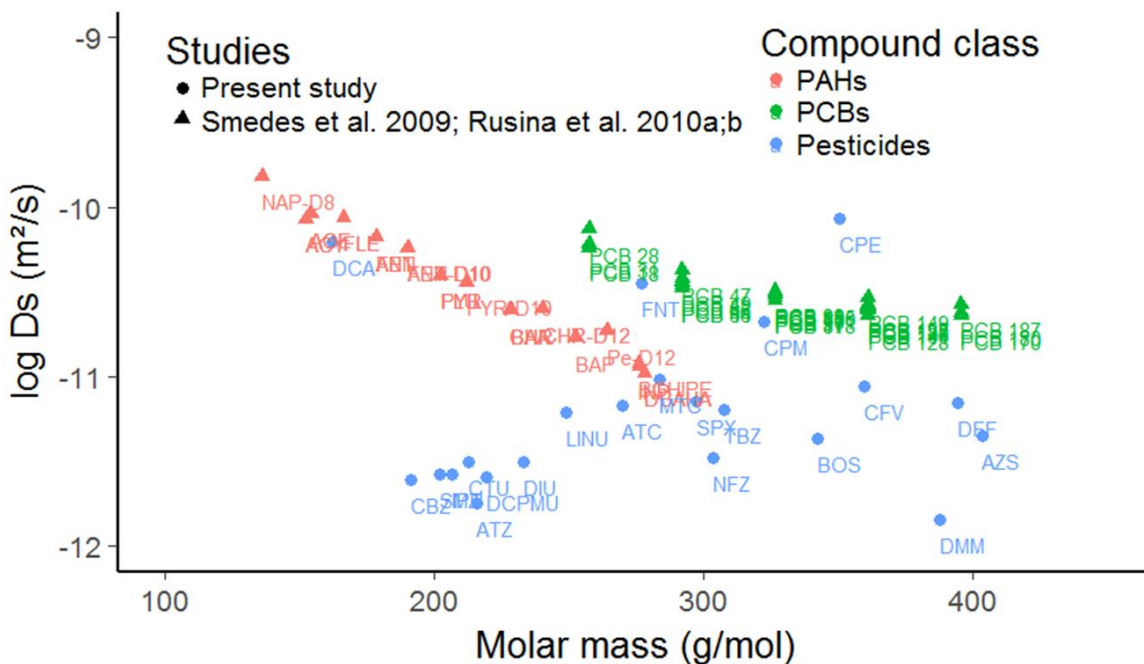
SI-5. Molecular properties (M , V_m , $\text{Log } D_w$) of pesticides.

Pesticide	M^a	V_m^a	$\text{Log } D_w^b$
	(g mol^{-1})	($\text{cm}^3 \text{mol}^{-1}$)	($\text{m}^2 \text{s}^{-1}$)
ATC	269.8	240.9	-9.28
ATZ	215.7	163.1	-9.18
AZS	403.4	300.1	-9.34
BOS	342.2	262.1	-9.3
CBZ	191.2	137.5	-9.14
CFV	359.6	261.8	-9.30
CPE	350.6	236.8	-9.28
CPM	322.5	203.8	-9.24
CTU	212.7	184.5	-9.21
DCA	162.0	115.6	-9.09
DCPMU	219.1	152.1	-9.16
DFE	394.3	274.0	-9.31
DIU	233.1	178.6	-9.21
DMM	387.9	315.1	-9.35
FNT	277.2	202.8	-9.24
IMD	255.7	160.1	-9.18
IPU	206.3	196.3	-9.23
LINU	249.1	185.2	-9.21
MTC	283.8	257.8	-9.30
NFZ	303.7	208.8	-9.24
PCM	284.1	189.1	-9.22
SMZ	201.7	147.9	-9.16
SPX	297.5	308.2	-9.34
TBZ	307.8	268.1	-9.31

^a Predicted by ACD/Labs: <http://www.chemspider.com/>

^b Calculated from Hayduk and Laudie (1974)

- 1 SI-6. Plot of $\log D_s$ versus molar mass (M) and molar volume (V_m) for PAHs and PCBs
- 2 (experimental values from Rusina et al. [2]) and for pesticides (estimated from this study).



4 **SI-7. Spreadsheet file compiling results from the two calibration experiments for 24**
5 **pesticides and 13 candidate PRCs at two flow velocities (5 and 20 cm·s⁻¹). Accumulated**
6 **mass of pesticides (*m*, ng) were not corrected by corresponding solvent back extraction**
7 **recoveries (Table 1). Concentrations of pesticides in water (*C_w*) was expressed in µg L⁻¹.**

8
9

10 References

- 11 [1] Martin A, Margoum C, Randon J, Coquery M. 2016. Silicone rubber selection for passive
12 sampling of pesticides in water. *Talanta* 160:306-313.
- 13 [2] Rusina TP, Smedes F, Klanova J. 2010. Diffusion Coefficients of Polychlorinated
14 Biphenyls and Polycyclic Aromatic Hydrocarbons in Polydimethylsiloxane and Low-Density
15 Polyethylene Polymers. *Journal of Applied Polymer Science* 116:1803-1810.
- 16 [3] Rusina TP, Smedes F, Koblizkova M, Klanova J. 2010. Calibration of silicone rubber
17 passive samplers: experimental and modeled relations between sampling rate and compound
18 properties. *Environmental Science & Technology* 44:362-367.
- 19
20